Optogenetic control of cell differentiation in channelrhodopsin-2-expressing OS3, a bipotential glial progenitor cell line

Kenji Ono, Hiromi Suzuki, Ryusei Yamamoto, Hideki Sahashi, Yuhei Takido, and Makoto Sawada

Department of Brain Function, Division of Stress Adaptation and Protection, Research Institute of Environmental Medicine, Nagoya University, Furo-cho, Chikusa-ku, Nagoya, Aichi 464-8601, Japan

*Correspondence and reprint requests should be addressed to: Dr. Hiromi Suzuki,

Department of Brain Function, Division of Stress Adaptation and Protection, Research Institute of Environmental Medicine, Nagoya University, Furo-cho, Chikusa-ku, Nagoya, Aichi 464-8601, Japan.

Tel.: +81-52-789-5002; fax: +81-52-789-3994; e-mail: hiromi_s@riem.nagoya-u.ac.jp

Abbreviations: ChR2, Channelrhodopsin-2; BL, blue light; OS3ChR2 cells, ChR2-expressing OS3 cells; GalC, galactocerebrosides; GFAP, glial fibrillary acidic protein; LPC, lysophosphatidyl choline; PDGF, platelet-derived growth factor; IGF-1, insulin-like growth factor 1; NT-3, neurotrophin-3; MEK, MAPK/ERK kinase; ERK, extracellular signal-regulated kinase; PI3K, phosphatidylinositol-3 kinase; Akt, protein kinase B; mTOR, mammalian target of rapamycin; p70 S6K, p70 S6 kinase; EYFP, enhanced yellow protein; MEM, Eagle's minimum essential medium; HEPES, 4-(2-hydroxyethyl)-1-piperazineethanesulfonic acid; RB, recording buffer; AM, acetoxymethyl; EGTA, ethylene glycol tetraacetic acid; BAPTA, 1,2-Bis(2-amino-5-methylphenoxy)ethane-N,N,N',N'-tetraacetic acid; PMSF, phenylmethylsulfonyl fluoride; PVDF, polyvinylidene difluoride; TBS, Tris-buffered saline; JNK, c-jun N-terminal kinase; PDK1, phosphoinositide-dependent protein kinase 1; PLP, proteolipid protein; Cx43, connexin 43; GLAST, glutamate aspartate transporter; GAPDH, glyceraldehyde-3-phosphate dehydrogenase; WST-1, 4-[3-(4-Iodophenyl)-2-(4-nitrophenyl)-2H-5-tetrazolio]-1,3-benzene disulfonate; BMS, Basso Mouse Scale for locomotion; PFA, paraformaldehyde; MAS, Matsunami adhesive silane; LFB, luxol fast blue; MAP-2, microtubule associated protein-2; PLC, phospholipase C; PKC, protein kinase C; BMP, bone morphogenetic protein; LIF, leukemia inhibitory factor

Abstract

Alterations in the intracellular ion environment have been identified as one of the signals playing a critical role in the control of cellular proliferation and differentiation; however, the mechanisms responsible for signal transduction remain unclear. Recent studies have reported that channelrhodopsin-2 (ChR2) is a rapidly gated blue light (BL)-sensitive cation channel suitable for the non-invasive control of ion influx. We herein examined the expression of differentiation-associated markers by photo-activation and its signal transduction in ChR2-expressing OS3 (OS3ChR2) cells, which are clonal bipotential glial progenitor cells. Increases were observed in intracellular Na^+ and Ca^{2+} concentrations in OS3ChR2 cells with BL exposure. Alterations in the intracellular ion environment, particularly in Ca^{2+}, led to increases in the expression of oligodendrocyte markers including galactocerebrosides (GalC) and decreases in that of astrocyte markers such as glial fibrillary acidic protein (GFAP). These alterations also triggered activation of the ERK1/2 signaling pathway, which is involved in cell survival, and PI3K/Akt/mTOR signaling pathway, which is involved in oligodendrocyte differentiation, characterized by GalC expression. Moreover, when photo-activated OS3ChR2 cells were injected into mice with lysophosphatidyl choline (LPC)-induced demyelination, deficits in motor function were reduced. Our results demonstrated that signal transduction by ChR2-expressing glial progenitor cells may be controlled through alterations induced in the intracellular ion environment by photo-activation and results in oligodendrocyte differentiation from glial progenitor cells. Our results also suggest that ChR2-expressing glial progenitor cells have potential as a useful tool for therapeutic approaches to brain and spinal cord disorders associated with oligodendrocyte dysfunctions.

Keywords: differentiation, oligodendrocyte, PI3K/Akt signaling, intracellular ion environment, channelrhodopsin-2, photo-activation

1. Introduction

A complex interplay of multiple extracellular and intracellular signals governs the balance between cell proliferation and differentiation. Alterations in the intracellular ion environment have been identified as one of these signals playing a critical role in the control of cellular proliferation and differentiation (Schreiber, 2005; Sontheimer, 1994). These alterations are also involved in oligodendrocyte differentiation from neural and glial progenitor cells. Oligodendrocyte lineages express multiple types of Ca^{2+} and Na^{+} channels, which are highly regulated in different stages of development (Paez et al., 2009). In glial progenitor cells, Ca^{2+} influx across the plasma membrane occurs through a number of routes such as ligand-operated channels (Hart et al., 1989), voltage-operated Ca^{2+} channels (Paez et al., 2007) and store-operated Ca^{2+} channels from Ca^{2+} stores in the endoplasmic reticulum (Alberdi et al., 2005). The expression of Na^{+} channels appears to be down-regulated as glial progenitor cells mature into differentiated oligodendrocytes (Berger et al., 1992; Sontheimer et al., 1989). Alterations in intracellular pH, which is regulated by movement of several ions such as Cl^{-}, HCO_3^{-}, Ca^{2+} and Na^{+} across the membrane, have been shown to trigger oligodendrocyte differentiation in primary cultures (Bernard et al., 2006; Boussouf and Gaillard, 2000). The intracellular ion environment such as Ca^{2+} and Na^{+} is involved in oligodendrocyte differentiation from glial progenitor cells; however, the mechanisms by which oligodendrocyte differentiation results from alterations in the intracellular ion environment have not yet been elucidated in detail.

Several growth factors such as platelet-derived growth factor (PDGF), insulin-like growth factor 1 (IGF-1), and neurotrophin-3 (NT-3) induce oligodendrocyte differentiation from neural progenitor and stem cells (Hu et al., 2004; McMorris et al., 1990; Raff et al., 1988). The MAPK/ERK kinase (MEK)/extracellular signal-regulated kinase (ERK) pathway and/or phosphatidylinositol-3 kinase (PI3K)/protein kinase B (Akt) pathway, which are activated by growth factors, promote

oligodendrocyte differentiation and myelination (Bibollet-Bahena and Almazan, 2009; Guardiola-Diaz et al., 2012). In addition, the mammalian target of rapamycin (mTOR), a well-known Akt substrate, regulates oligodendrocyte differentiation and myelination via the phosphorylation of p70 S6 kinase (p70 S6K) (Narayanan et al., 2009; Tyler et al., 2009). A PDGF stimulation was previously shown to not only activate signal transduction, but also enhance Ca^{2+} influx in glial progenitor cells (Paez et al., 2010). Oligodendrocyte differentiation induced by intracellular pH, which is closely involved in intracellular Na^{+} concentrations, is controlled via ERK1/2 pathway activation (Bernard et al., 2006). Thus, alterations in the intracellular ion environment may trigger the MEK/ERK pathway and PI3K/Akt pathway and result in oligodendrocyte differentiation.

A bipotential glial progenitor cell line from the mouse cerebrum, designated OS3, phenotypically differentiates into oligodendrocytes and astrocytes both *in vitro* and *in vivo* (Ohtani et al., 1992; Sawamura et al., 1995). OS3 cells are morphologically similar to astrocytes when grown in the presence of 10% serum. Under these culture conditions, OS3 cells immunohistochemically express glial fibrillary acidic protein (GFAP), which is one of the representative markers for astrocytes. When OS3 cells are cultured in low serum-containing medium or chemically defined medium, they lose immunoreactivity for GFAP and differentiate into oligodendrocytes, which express specific markers for oligodendrocyte lineages such as galactocerebrosides (GalC).

Recent studies have reported that channelrhodopsin-2 (ChR2) is a rapidly gated BL-sensitive cation channel suitable for the non-invasive control of ion influx (Zhang et al., 2007). Since it is useful for the control of neuronal spiking and synaptic transmission in ChR2-expressing neurons with BL, ChR2 has become a powerful tool in neural circuit analyses. Moreover, ChR2 functions in glial cells that cannot generate action potentials, unlike neurons (Figueiredo et al., 2011; Ono et al., 2014). Although it currently remains unclear whether ChR2 functions in glial progenitor cells such as OS3

cells, if ChR2 on glial progenitor cells has the ability to control the intracellular ion environment by photo-activation, glial progenitor cells may differentiate into oligodendrocytes.

We herein demonstrated that ChR2-expressing OS3 (OS3ChR2) cells, which are clonal bipotential glial progenitor cells, successfully differentiated into GalC-expressing oligodendrocytes through increases in intracellular cations, particularly Ca^{2+}, by photo-activation. The increase in intracellular cations by photo-activation triggered activation of the PI3K/Akt pathway in OS3ChR2 cells and was associated with oligodendrocyte differentiation.

2. Materials and Methods

2.1. Cell lines

OS3 murine glial progenitor cell lines, including ChR2-EYFP (enhanced yellow protein)-expressing derivatives, were cultured in Eagle's Minimum Essential Medium (MEM) (Sigma-Aldrich, St Louis, MO, USA) supplemented with 10% fetal bovine serum, 5 μg/ml of bovine insulin (Sigma-Aldrich), 2% of glucose (Sigma-Aldrich), and Penicillin-Streptomycin (Life Technologies, Carlsbad, CA, USA) in a 95% air/5% CO_2-humidified atmosphere.

2.2. Plasmids and Electroporation

The pcDNA3.1/hChR2-EYFP plasmids used were a generous gift from Dr. Karl Deisseroth (Stanford University). OS3 cells (1 x 10^6 cells/400 μl) were mixed with 10 μg of plasmids in a 4-mm gap cuvette. The cuvette was set in an ECM830 electroporator (BTX Instrument Division Harvard Apparatus, Inc., Holliston, MA, USA) and electroporation was performed under the following conditions (LV mode, 170 V, 70 ms pulse length, single pulse). Transfected cells were cultured in medium with 600 μg/ml of G418 for the selection of mixed clones expressing ChR2-EYFP for 7 days. Several kinds of single clones were picked up from mixed clones after limiting dilutions and a single clone was used in this study.

2.3. Time-lapse fluorescent imaging

Time-lapse series of cells were taken as described previously (Ono et al., 2014). In brief, the CoroNa Red fluorescent probe (Life Technologies) was used to visualize the influx of Na^+. CoroNa Red, which is a sodium indicator and increases red fluorescence in a concentration-dependent manner, was loaded onto OS3 cells and OS3ChR2 cells at 1 μM in recording buffer (RB) containing 137 mM sodium chloride, 4.2 mM sodium carbonate, 0.34 mM disodium hydrogen phosphate, 5.4 mM potassium chloride, 0.44 mM potassium dihydrogen phosphate, 0.81 mM magnesium sulfate, 1.26 mM calcium chloride, 5.55 mM D-glucose, and 20 mM HEPES (pH7.4) for 30 min. After removing

over-loaded CoroNa Red, time-lapse series of cells were taken in RB for 10 min. BL was applied for 200 ms every 30 s. The Rhod-3 Imaging Kit (Life Technologies) was used to visualize the influx of Ca^{2+}. Rhod-3AM, which is a calcium indicator that increases red fluorescence in a concentration-dependent manner, was loaded onto OS3 cells and OS3ChR2 cells at 10 μM in RB for 30 min. After removing over-loaded Rhod-3 AM, cells were incubated in RB containing 2.5 mM probenecid, which aided AM ester dye-loading and retention in the cells. Time-lapse series of cells were taken in RB for 10 min. BL was applied for 500 ms every 30 s. Fluorescent intensity from the time-lapse series was measured using Image-Pro Plus software (Media Cybernetics, Inc., Bethesda, MD, USA). In some cases, time-lapse series of cells were taken in RB supplemented with 100 μM EGTA, 10 μM BAPTA-AM and 1 μM ionomycin or in sodium ion-free buffer containing 137 mM choline chloride, 5 mM potassium chloride, 2 mM calcium chloride, 1 mM magnesium sulfate, and 10 mM HEPES (pH7.4). For long-term BL exposure, cells were cultivated for 24 h and exposed to BL in the medium for 1min every 5 min until 72 h at 37 °C in 5 % CO_2 using the Safe Imager Blue-Light Transilluminator (LED light source producing a single-intensity signal at approximately 470 nm, Life Technologies). At the start or the end of BL exposure, cells were labeled with CoroNa Red or Rhod-3 and taken photographs using fluorescent microscope. Ratio of fluorescent intensity before and after BL exposure was measured using Image-Pro Plus software.

2.4. Western blotting

In order to detect phosphorylation, OS3 or OS3ChR2 cells were plated on a 100-mm Cell Culture Dish at a density of 1.0 x 10^6 cells and cultivated for 72 h. Culture medium was exchanged to serum-free MEM and serum-starved overnight. Cells were pretreated with 100 μM EGTA, 10 μM BAPTA-AM, 1 μM U0126, 10 μM LY294002, 1 μM Triciribine, 1 μM BX-517, or 50 nM rapamycin at 30 min before BL exposure for the inhibition of signal transduction. Cells in medium were exposed to BL for 1 min every 5 min until 24 h at 37 °C in 5 % CO_2 using the Safe Imager

Blue-Light Transilluminator. In order to detect protein expression, OS3 or OS3ChR2 cells were plated on a 100-mm Cell Culture Dish at a density of 1.0 x 10^6 cells and pretreated with 100 μM EGTA, 10 μM BAPTA-AM, 1 μM U0126, 10 μM LY294002, 1 μM Triciribine, 1 μM BX-517, or 50 nM rapamycin at 30 min before BL exposure. Cells in medium were exposed to BL for 1 min every 5 min until 72 h using the Safe Imager Blue-Light Transilluminator. A fraction of cells were used for FACS analysis. Cells were lysed in Cell Lysis Buffer (20 mM Tris-HCl, 150 mM NaCl, 1 mM Na_2EDTA, 1 mM EGTA, 1% Triton, 2.5 mM sodium pyrophosphate, 1mM β-glycerophosphate, 1 mM Na_3VO_4, 1 μg/ml leupeptin, pH 7.5) (Cell Signaling Technology, Danvers, MA) containing additional protease and phosphatase inhibitors (1 mM PMSF, Phosphatase Inhibitor Cocktail 2, Phosphatase Inhibitor Cocktail 3 (Sigma-Aldrich)) by sonication on ice. Lysates were stored at -80°C prior to the Western analysis. The BCA Protein Assay (Thermo Fisher Scientific, Rockford, IL) was performed in order to determine protein concentrations. Twenty micrograms of total protein per sample was aliquoted, mixed with loading buffer (Cell Signaling Technology), boiled for 5 min, and separated by SDS-PAGE on mini-gels (Oriental Instruments, Kanagawa, Japan). Separated proteins were then transferred to PVDF (polyvinylidene difluoride) membranes on an iBlot Gel Transfer Device (Life Technologies) and blocked in 5% nonfat dry milk (Cell Signaling Technology)/TBS (Tris-buffered saline)-0.1% Tween at room temperature for 1 h. Membranes were then incubated in the presence of primary antibodies diluted in 5% nonfat dry milk/TBS-0.1% Tween at a 1:2000 dilution at 4°C overnight. Primary antibodies directed against GFP (Medical & Biological Laboratories Co., Ltd., Nagoya, Japan), phospho-ERK1/2 (Thr202/Tyr204) (Cell Signaling Technology), phospho-p38 MAPK (Thr180/Tyr182) (Cell Signaling Technology), phospho-c-jun N-terminal kinase (JNK) (Thr183/Tyr185) (Cell Signaling Technology), phospho-Akt (Thr308) (Cell Signaling Technology), phospho-Akt (Ser473) (Cell Signaling Technology), phospho-phosphoinositide-dependent protein kinase 1 (PDK1) (Ser241) (Cell Signaling Technology),

phospho-mTOR (Ser2448) (Cell Signaling Technology), phospho-p70 S6K (Thr389) (Cell Signaling Technology), phospho-p70 S6K (Ser371) (Cell Signaling Technology), GalC (Sigma-Aldrich), and GFAP (Sigma-Aldrich) were used. The following day, membranes were washed 5 times for 8 min with TBS-0.1% Tween and incubated at room temperature for 1 h in 5% nonfat dry milk/TBS-0.1% Tween containing HRP-conjugated secondary antibodies (Cell Signaling Technology) at a 1:5000 dilution. Protein was visualized by chemiluminescence using ECL Prime (GE Healthcare, Little Chalfont, UK) and Light Capture II (Atto, Tokyo, Japan). In the case of a faint signal being detected, primary and secondary antibodies were diluted in Can Get Signal Immunoreaction Enhancer Solution (Toyobo, Osaka, Japan) instead of 5% nonfat dry milk/TBS-0.1% Tween. In order to normalize for sample loading and protein transfer, the membranes were stripped and reprobed with an antibody for ERK1/2 (Cell Signaling Technology), p38 MAPK (Cell Signaling Technology), JNK (Cell Signaling Technology), total Akt (Cell Signaling Technology), PDK1 (Cell Signaling Technology), mTOR (Cell Signaling Technology), or GAPDH (Millipore, Billerica, MA) as indicated. Molecular weight and signal intensity were analyzed using CS Analyzer software (Atto).

2.5. RNA extraction and Real-time PCR

Total RNA extraction and cDNA synthesis were performed as described previously (Ono et al., 2014). cDNA was amplified and analyzed with Power SYBR Green PCR Master Mix and 7900 Real-Time PCR System (Applied Biosystems, Tokyo, Japan) using primer pairs specific to the proteolipid protein (PLP; sense primer: TCA GTC TAT TGC CTT CCC TAG C; antisense primer: AGC ATT CCA TGG GAG AAC AC), Olig2 (sense primer: CTT CAC AGG AGG GAC TGT GTC; antisense primer: GGT GCT GGA GGA AGA TGA CT), GFAP (sense primer: CGC TTC TCC TTG TCT CGA AT; antisense primer: TGT AGC TAG CAA AGC GGT CA), connexin 43 (Cx43; sense primer: TCC TTG GTG TCT CTC GCT CT; antisense primer: TTT GGA GAT CCG CAG TCT TT), glutamate aspartate transporter (GLAST; sense primer: ACA TGT TCC CTC CCA ATC TG;

antisense primer: AGA GTC TCC ATG GCC TCT GA), or glyceraldehyde-3-phosphate dehydrogenase (GAPDH; sense primer: TGC ACC ACC AAC TGC TTA G; antisense primer: GAT GCA GGG ATG ATG TTC) for 40 cycles (95 °C for 15 s, 60 °C for 60 s). mRNA expression for differentiation markers was analyzed by the Delta-Delta Ct method (Bubner et al., 2004) and the ratio of PLP, Olig2, GFAP, Cx43 or GLAST to GAPDH was calculated.

2.6. FACS analysis

EYFP fluorescence and expression of GalC and GFAP in OS3ChR2 cells were detected using a FACSCalibur cell sorter (BD Bioscience, San Jose, CA, USA) and CellQuest software (BD Bioscience). Cells were fixed with 4 % paraformaldehyde (PFA) in PBS (pH 7.2) at room temperature for 10 min, permeabilized in PBS containing 0.1 % Triton X-100 for 10 min, and blocked with a blocking buffer (1 % bovine serum albumin, 10 % normal goat serum, and 0.05 % sodium azide) for 30 min on ice. Cells were incubated with antibodies against GalC and GFAP at a dilution of 1:200 on ice, and then visualized with Alexa647-conjugated goat anti-rabbit IgG or anti-mouse IgG (Life Technologies)

2.7. WST assay

Cell proliferation was determined using the WST-1 Cell Counting Kit (Dojindo Laboratories, Kumamoto, Japan). WST-1 (light red) is cleaved to its formazan derivate (dark red) by mitochondrial enzyme in viable cells and the absorbance of formazan derivate is in directly proportion to the number of viable cells. OS3ChR2 cells were plated on 96-well culture plates at a density of 5 x 10^3 cells / 100 μl culture medium and cultured in the presence or absence of U0126 (0 nM-10 μM) with or without BL exposure for 24 h or 72 h. Each plate was exposed to BL for 1 min every 5 min until 72 h using the Safe Imager Blue-Light Transilluminator at 37 °C in 5% CO_2. At the end of the experiments, cells were incubated with 10 μl of the WST-1 reagent for 4 h. Absorbance was

measured at 450 nm and 620 nm (as a reference) using a micro plate reader (GE Healthcare, Chalfont St. Giles, United Kingdom).

2.8. Cell viability

OS3ChR2 cells were plated on a 60-mm Cell Culture Dish at a density of 2.0 x 10^5 cells and pretreated with U0126 (0 nM-10 μM) for 30 min before BL exposure. Cells in medium were exposed to BL for 1 min every 5 min until 72 h using the Safe Imager Blue-Light Transilluminator. All cells were collected after trypsinization and 10 μl of the cell suspension was mixed with the same volume of trypan blue. Cell viability was measured from the mixture using a Countess Automated Cell Counter (Life Technologies).

2.9. Motor function test

To induce demyelination, C57BL/6 mice were treated with LPC (Sigma-Aldrich). Briefly, C57BL/6 mice were anesthetized with isoflurane and the thoracic vertebrae were exposed. 1 mm burr holes were drilled and 2 μl of LPC (1%) dissolved in PBS was injected into dorsal column by a 10 μl Hamilton syringe. At 3 days after LPC treatment, OS3ChR2 cells (1 x 10^6 cells/mouse) with or without BL for 1 min every 5 min until 72 h using the Safe Imager Blue-Light Transilluminator were injected into dorsal column by the Hamilton syringe. At 1, 7 and 14 days after the cell injection, recovery of hindlimb motor function was scored by the Basso Mouse Scale for locomotion (BMS) (Basso et al., 2006) and motor coordination and balance were tested using a rota-rod (MK-610, Muromachi Kikai Co., Ltd., Tokyo, Japan). BMS results in scores ranging from 0 (complete paralysis) to 9 (normal mobility). For the rota-rod test, all mice were allowed trial run on the rod three times a day for 3 days before LPC treatment to get used to rota-rod. Mice were set on the rod and the velocity of the rod was increased from 0 rpm to 40 rpm during 60 s and kept at 40 rpm. Latency until fall was recorded. Mice were given a maximum cutoff latency of 120 s to minimize stress and fatigue.

2.10. Immunohistochemical analysis

At 2 weeks after the cell injection, mice were transcardially perfused with 4 % PFA in PBS. The spinal cords were post-fixed for 24 h at 4 °C, followed by immersion in 30 % sucrose in PBS at 4 °C until they were equilibrated. They were embedded in Tissue-Tek OCT compound (Sakura Finetek Japan Co. Ltd., Tokyo, Japan) and stored at –80 °C. Spinal cord sections (10 μm) were serially cut with a cryostat microtome (Leica Biosystems, Nussloch, Germany), then transferred to MAS (Matsunami adhesive silane)-coated slides (Matsunami Glass Ind., Ltd., Osaka, Japan) and air-dried. For luxol fast blue (LFB) staining, the sections were washed with 95 % ethanol, and incubated with LFB solution (Muto pure chemicals Co., Ltd., Tokyo, Japan) at 60 °C overnight. The sections were decolorized using 0.05 % lithium carbonate solution (Muto pure chemicals Co., Ltd.) and 70 % ethanol. After dehydration, spinal cords were observed using a microscope equipped with DP70 digital camera (Olympus Co., Ltd., Tokyo, Japan). For immunofluorescent staining, the sections were treated with 0.1% triton-X for 10 min for improvement of permeability and then incubated with the blocking buffer for 30 min. The sections were multiply labelled with monoclonal antibodies against MAP-2 (microtubule associated protein-2; Millipore) at a dilution of 1:200 and polyclonal antibodies against GFP (green fluorescent protein; MBL) at a dilution of 1:500. The reaction was visualized with Alexa546-conjugated goat anti-mouse IgG (Life Technologies) at a dilution of 1:500 and Alexa488 conjugated goat anti-rabbit IgG (Life Technologies) at a dilution of 1:400. Fluorescent images were captured with an imaging system (Apotome; Carl Zeiss, Oberkochen, Germany).

2.11. Statistical analysis

Statistical analyses were performed using a 2-tailed *t*-test or one-way ANOVA and Tukey post hoc tests. Differences were considered significant when the p value was less than 0.05.

3. Results

3.1. OS3 cells transfected with the ChR2-EYFP gene (OS3ChR2 cells)

In order to clarify the expression of the ChR2-EYFP fusion protein, OS3ChR2 cells were analyzed using a flow cytometer (Fig. 1A). EYFP-specific fluorescence was detected in OS3ChR2 cells. Furthermore, the ChR2-EYFP fusion protein was detected in OS3ChR2 cells by Western blotting (Fig. 1B). An approximately 60 kDa band of the ChR2-EYFP fusion protein was clearly observed in OS3ChR2 cells.

3.2. Na^+ and Ca^{2+} influx in OS3ChR2 cells by BL exposure.

In an attempt to determine whether ChR2 functioned on OS3ChR2 cells with BL exposure, intracellular Na^+ concentrations were monitored using a CoroNa Red fluorescent probe, which is a Na^+ indicator and increases red fluorescence in an intracellular Na^+ concentration-dependent manner. Although intracellular fluorescence did not increase in OS3 cells with BL exposure, it significantly increased in OS3ChR2 cells (Fig. 2A and B). Intracellular Ca^{2+} concentrations were then monitored by a Rhod-3 fluorescent probe, which is a Ca^{2+} indicator. Intracellular fluorescence appeared to increase in OS3ChR2 cells with BL (Fig. 2C and D). In order to confirm whether the influx of Na^+ and Ca^{2+} was from the extracellular fluid, increases in CoroNa Red fluorescence and Rhod-3 fluorescence in photo-activated OS3ChR2 cells were observed in Na^+-free buffer or calcium chelator-containing buffer such as EGTA (an extracellular calcium chelator) and BAPTA-AM (an intracellular calcium chelator) (Fig. 2E and F). Increases in CoroNa Red fluorescence in photo-activated OS3ChR2 cells were not observed in Na^+-free buffer (Fig. 2E), which indicated the influx of Na^+ was from the extracellular fluid. Furthermore, increases in Rhod-3 fluorescence in photo-activated OS3ChR2 cells were not observed in EGTA-containing buffer as well as BAPTA-AM-containing buffer (Fig. 2F), which also indicated that the influx of Ca^{2+} was from the extracellular fluid. Increases in CoroNa Red fluorescence in photo-activated OS3ChR2 cells were

not affected in EGTA-containing buffer (Fig. 2E), whereas those in Rhod-3 fluorescence were not observed in Na^+-free buffer (Fig. 2F). These results suggest that the influx of Na^+ through photo-activated ChR2 triggered the influx of Ca^{2+} in OS3ChR2 cells. Moreover, in an attempt to confirm whether concentration of intracellular Na^+ and Ca^{2+} increased in OS3ChR2 cells after lasting BL exposure, increases in CoroNa Red and Rhod-3 fluorescence were examined in photo-activated OS3ChR2 cells during 72 h with BL exposure (Fig. 2G). Increases in intracellular Na^+ and Ca^{2+} were kept until 72 h with BL exposure.

3.3. Differentiation of OS3ChR2 cells into oligodendrocytes by photo-activation.

In order to clarify whether alterations in the intracellular ion environment were involved in cell differentiation, we examined mRNA expression for differentiation markers in OS3 cells and OS3ChR2 cells by photo-activation (Fig. 3A). PLP and Olig2 mRNA expression, which are markers of differentiation into oligodendrocytes, was significantly increased in OS3ChR2 cells, but not in OS3 cells by photo-activation, whereas the expression of GFAP, Cx43, and GLAST mRNA, which are markers of differentiation into astrocytes, appeared to be decreased. GalC and GFAP protein expression in OS3 and OS3ChR2 cells was analyzed by FACS analysis and Western blotting (Fig. 3B and C). GalC expression in OS3ChR2 cells appeared to be increased by photo-activation, while GFAP expression was decreased, whereas no changes were observed in GalC or GFAP expression in OS3 cells by photo-activation. These results suggest that OS3ChR2 cells differentiate into oligodendrocytes, but not astrocytes by activated ChR2. Since intracellular Ca^{2+} concentrations in OS3ChR2 cells were increased by photo-activation as shown in Figure 2, we investigated whether GalC and GFAP expression in photo-activated OS3ChR2 cells was altered in the presence of EGTA and BAPTA-AM, extracellular and intracellular chelators of Ca^{2+} (Fig. 3D and E). Increases in the expression of GalC in photo-activated OS3ChR2 cells were significantly blocked in the presence of EGTA and BAPTA-AM. Moreover, the expression of GFAP in these cells was conversely increased.

Therefore, alterations in intracellular Ca^{2+} concentrations via photo-activated ChR2 appeared to trigger the differentiation of OS3ChR2 cells into oligodendrocytes.

3.4. Phosphorylation of ERK1/2 in OS3ChR2 cells by photo-activation.

The ERK1/2 and PI3K/Akt pathways are involved in oligodendrocyte differentiation (Guardiola-Diaz et al., 2012). In order to establish whether alterations in the intracellular ion environment activate signal transduction, we examined the phosphorylation of MAPKs such as ERK1/2, p38 MAPK, and JNK in OS3ChR2 cells by photo-activation. The phosphorylation of ERK1/2 on Thr202/Tyr204 increased in a time-dependent manner (Fig. 4A), whereas that of p38 MAPK on Thr180/Tyr182 and JNK on Thr183/Tyr185 was not detected. In order to inhibit the phosphorylation of ERK1/2, OS3ChR2 cells were treated with U0126 (1 μM), a selective inhibitor of MEK1 and MEK2, which are upstream kinases that phosphorylate ERK1/2. Although U0126 slightly blocked the phosphorylation of ERK1/2 in OS3ChR2 cells by photo-activation (Fig. 4B), no changes were observed in the increases in GalC protein expression in OS3ChR2 cells induced by photo-activation (Fig. 4C). To confirm whether the increases in intracellular Ca^{2+} were involved in phosphorylation of ERK1/2, phosphorylation of ERK1/2 was examined in photo-activated OS3ChR2 cells in the presence of EGTA or BAPTA-AM. The phosphorylation of ERK1/2 was not inhibited in the presence of EGTA (Fig. 5A), but BAPTA-AM (Fig. 5B). These results indicated that the phosphorylation of ERK1/2 in OS3ChR2 cells by photo-activation was not involved in the increase observed in GalC expression. To clarify its phosphorylation, we compared the WST reduction activity, an indicator of cell number, of OS3ChR2 cells on Days 1 and 3 in the absence or presence of U0126 with and without BL exposure (Fig. 5C). The WST reduction activity of OS3ChR2 cells was significantly decreased on Days 1 and 3 by BL exposure. Furthermore, WST reduction activity was markedly decreased by the additional treatment of U0126 at a dose of more than 2 μM. In order to confirm whether the decrease observed in WST reduction activity on Days 1

and 3 was due to a reduced proliferative capacity or cell death, OS3ChR2 cells exposed to BL for 3 days were stained with trypan blue and their viability was measured (Fig. 5D). No significant differences were noted in the ratio of dead cells in OS3ChR2 cells with or without BL exposure; however, cell death was induced in most OS3ChR2 cells exposed to BL by the additional treatment with U0126 at a dose of more than 2 μM, but not in those without BL exposure. These results suggest that the phosphorylation of ERK1/2 in OS3ChR2 cells by photo-activation is required for cell growth and survival, but not cell differentiation.

3.5. Phosphorylation of Akt in OS3ChR2 cells by photo-activation.

We examined the phosphorylation of Akt in photo-activated OS3ChR2 cells in order to clarify whether alterations in the intracellular ion environment activate other signal transduction pathways. The phosphorylation of Akt on Thr308 and Ser473 increased in a time-dependent manner (Fig. 6A). In addition, the phosphorylation of PDK1 on Ser241, which phosphorylates Akt on Thr308, also increased in a time-dependent manner. In order to confirm that increases in the influx of Ca^{2+} in photo-activated OS3ChR2 cells were involved in the phosphorylation of Akt and PDK1, we examined their phosphorylation in the presence of EGTA (Fig. 6B) or BAPTA-AM (Fig. 6C). The phosphorylation of Akt in OS3ChR2 cells by BL exposure was strongly blocked, whereas that of PDK1 was partially inhibited in the presence of EGTA. In addition, the phosphorylation of Akt and PDK1 in photo-activated OS3ChR2 cells was strongly blocked in the presence of BAPTA-AM. These results demonstrated that increases in intracellular Ca^{2+} concentrations in OS3ChR2 cells were involved in the activation of the Akt signaling pathway. In order to confirm the activation of the Akt signaling pathway by photo-activation, the phosphorylation of Akt on Thr308 and Ser473 was examined in photo-activated OS3ChR2 cells in the presence of LY294002 (10 μM), a PI3K inhibitor, Triciribine (1 μM), an Akt inhibitor, or BX-517 (1 μM), a PDK1 inhibitor (Fig. 7A). The phosphorylation of Akt in OS3ChR2 cells by BL exposure was significantly inhibited in the presence

of inhibitors for upstream kinases such as PI3K and PDK1 as well as an inhibitor for Akt. The protein expression of GalC and GFAP in OS3ChR2 cells was then analyzed in the presence of LY294002, Triciribine, or BX-517 by Western blotting (Fig. 7B). Increases in GalC protein expression in OS3ChR2 cells by photo-activation appeared to be inhibited in the presence of LY294002, Triciribine, and BX-517. On the other hand, no marked changes were noted in decreases in GFAP protein expression by photo-activation in the presence of their inhibitors; however, GFAP expression in OS3ChR2 cells without BL appeared to be decreased in the presence of LY294002 and Triciribine. These results indicate that the PI3K/Akt signaling pathway plays important roles in the differentiation of OS3ChR2 cells into oligodendrocytes via photo-activated ChR2.

3.6. Phosphorylated Akt by photo-activation triggered mTOR and p70 S6K activation.

The activation of mTOR, which is phosphorylated by Akt, is essential for the differentiation of glial progenitor cells into oligodendrocytes (Tyler et al., 2009). mTOR forms two distinct signaling complexes, termed mTORC1 and mTORC2, and rapamycin inhibits the kinase activity of mTOR in mTORC1 but not in mTORC2 (Jacinto et al., 2004). The phosphorylation of mTOR on Ser2448 in OS3ChR2 cells was examined in order to determine whether it is a substrate for phosphorylated Akt. The phosphorylation of mTOR in OS3ChR2 cells was increased by photo-activation, but was completely inhibited by the treatment with rapamycin (50 nM) (Fig. 8A). In addition, the increase observed in GalC expression in OS3ChR2 cells by photo-activation was also inhibited in the presence of rapamycin (Fig. 8B). Since p70 S6K is known as a substrate that activates mTORC1 in oligodendrocyte differentiation (Tyler et al., 2009), its phosphorylation on Thr389 and Ser371 in OS3ChR2 cells was examined (Fig. 8C). The phosphorylation of p70 S6K on both sites in OS3ChR2 cells was increased by photo-activation, but was completely blocked in the presence of rapamycin. These results suggest that Akt signaling activation in OS3ChR2 by photo-activation results in oligodendrocyte differentiation via the activation of mTORC1 and p70 S6K.

3.7. Photo-activated OS3ChR2 cells recovered demyelination

To confirm GalC-expressing OS3ChR2 cells by photo-activation functioned as oligodendrocytes, photo-activated OS3ChR2 cells were injected into demyelinated spinal cord in LPC treated mice. At 2 weeks after cell injection, motor functional recovery was significantly observed in mice, which were injected photo-activated OS3ChR2 cells (Fig. 9A and B). In the spinal cord, demyelinated region was decreased (Fig. 9C). In addition, many OS3ChR2 cells were not only attached to neurons but also wrapped them like myelin (Fig. 9D). Moreover, OS3ChR2 cells kept GalC expression in spinal cord at 2 weeks after injection (Fig. 9E).

4. Discussion

In the present study, we demonstrated that the forced expression of ChR2 in OS3 glial progenitor cells functioned as a cation channel that regulated the influx of Na^+ and Ca^{2+} by BL exposure. Alterations in the intracellular ion environment via cation influx in OS3ChR2 glial progenitor cells triggered the activation of the PI3K/Akt/mTOR pathway and resulted in oligodendrocyte differentiation, which is characterized by GalC expression and motor functional recovery. Oligodendrocytes, a type of glial cell in the central nervous system, insulate axons by creating myelin sheaths, which reduce ion leakage and increase impulse speed, and also have a supporting role for neurons (Nave, 2010). Since several diseases and traumas such as multiple sclerosis, leukodystrophies, and spinal cord injury induce cell death, demyelination, and dysfunctions in oligodendrocytes and result in abnormalities in neuronal transduction, therapeutic approaches using transplantation and the control of differentiation from neural progenitor and stem cells are desired. ChR2-expressing glial progenitor cells may activate intracellular signal transduction and differentiate into oligodendrocytes by photo-activation without additional ligands such as PDGF, IGF-1, and NT-3. Since the differentiation of oligodendrocytes from ChR2-expressing neural progenitor cells may be controlled by BL exposure, ChR2-expressing neural stem and progenitor cells may become a powerful tool for therapeutic approaches against brain and spinal cord disorders associated with oligodendrocyte dysfunctions.

In the present study, the deprivation of Na^+, but not Ca^{2+} from culture media prevented increases in intracellular Na^+ concentrations in photo-activated OS3ChR2 cells, indicating that these increases were due to the influx of Na^+ from the extracellular environment. The deprivation of Na^+ or Ca^{2+} prevented increases in intracellular Ca^{2+} concentrations in photo-activated OS3ChR2 cells, suggesting that increases in Ca^{2+} concentrations were due to the influx of Ca^{2+} from the extracellular environment triggered by the influx of Na^+.

Our results showed that increases in intracellular Ca^{2+} concentrations by photo-activation resulted in the activation of the PI3K/Akt/mTOR signaling pathway in OS3ChR2 cells. A recent study also reported that elevations in intracellular Ca^{2+} concentrations via calcium-permeable AMPA receptors were involved in the activation of PI3K in oligodendrocyte lineage cells (Zonouzi et al., 2011); however, the intermediate pathways from increases in intracellular Ca^{2+} concentrations to PI3K and its downstream activation remain unclear. A large number of calcium-binding proteins such as phospholipase C (PLC), protein kinase C (PKC), and calmodulin have been identified in neural cells (Drouva et al., 1991; Solà et al., 1999). PKC isoenzymes are phosphorylated by activated PDK1, one of the substrates for PI3K (Le Good et al., 1998). In addition, the PLC-PKC cascade is required for ERK and PI3K/Akt activation by IL-1β treatments (Amin et al., 2003); therefore, PLC and PKC signaling may be involved in the differentiation of ChR2-expressing glial progenitor cells into oligodendrocytes by photo-activation. Although the phosphorylation of the PI3K/Akt and MEK/ERK pathways was previously reported to increase or peak within 2 h in many cases when glial progenitor cells were treated with growth factors (Bibollet-Bahena and Almazan, 2009; Cui and Almazan, 2007), our results showed that the phosphorylation of Akt, PDK1, and ERK1/2 by photo-activation occurred slowly and increased from 6h. These results suggest the involvement of other pathways in this mechanism; therefore, further investigations are warranted in order to obtain more information.

Several studies have implicated the MEK/ERK and PI3K/Akt/mTOR pathways in the proliferation, migration, and survival of glial progenitor cells, largely as a result of their activation by various growth factors (Baron et al., 2000; Cui and Almazan, 2007; Flores et al., 2000; Frost et al., 2009; Heinrich et al., 1999; Van't Veer et al., 2009). However, information on the role of these signaling molecules in the differentiation of glial progenitor cells to mature oligodendrocytes is often contradictory. Baron et al. reported the inhibition of differentiation using MEK inhibitors (Baron et

al., 2000), whereas Fyffe-Maricich et al. found no inhibition or only the transient and partial inhibition of oligodendrocyte differentiation in mixed primary cortical cultures from Erk1-null or Erk2 conditional single knockout mouse brains, respectively (Fyffe-Maricich et al., 2011). In addition, Tyler et al. showed that the differentiation of glial progenitor cells to GalC-expressing oligodendrocytes was inhibited by rapamycin (Tyler et al., 2009), whereas Baron et al. found no inhibition at the same stage of the oligodendrocyte lineages using PI3K inhibitors (Baron et al., 2000). Our results demonstrated that the phosphorylation of PI3K/Akt was involved in oligodendrocyte differentiation, while that of ERK1/2 played a role in cell survival by photo-activated ChR2. Some of the discrepancies between our results and previous findings may be attributed to differences in the treated conditions, including growth factors and inhibitors, as well as the sources and stages of glial progenitor cells (Guardiola-Diaz et al., 2012).

Our results showed that the expression of GalC in OS3ChR2 cells was increased by photo-activation through the PI3K/Akt/mTOR signaling pathway. Furthermore, activated mTOR resulted in phosphorylation of p70 S6K as rapamycin inhibited phosphorylation of p70 S6K on Thr389 and Ser371 by mTOR. p70 S6K is a downstream effector that phosphorylates the S6 ribosomal protein, which controls protein synthesis at ribosomes. Thus, the expression of GalC may be controlled by the activation of p70 S6K in glial progenitor cells.

The expression of GFAP in OS3ChR2 cells was decreased by photo-activation, but was markedly increased in the presence of EGTA and BAPTA-AM by photo-activation. This result indicates that the expression of GFAP affects intracellular Ca^{2+} concentrations when OS3ChR2 cells are exposed to BL. The decrease observed in GFAP expression in OS3ChR2 cells by photo-activation remained or decreased further in the presence of U0126, LY294002, and Triciribine. The ERK1/2 and PI3K/Akt signaling pathways are involved in the expression of GFAP in neural cells (Chipoy et al., 2004; Dore et al., 2009; Peltier et al., 2007). Signaling by the TGF-β family including bone

morphogenetic protein (BMP) and IL-6 family such as leukemia inhibitory factor (LIF) promotes the differentiation of neural stem/progenitor cells into GFAP immunoreactive cells (Bonaguidi et al., 2005). PI3K has been shown to control STAT3 and Smad1/5/8 signaling by BMP and LIF, leading to astrogliogenesis and GFAP expression (Herrera et al., 2010). In addition, radial glia differentiation into astrocytes using TGF-β1 is mediated by the activation of the ERK1/2 signaling pathway (Stipursky et al., 2012). Therefore, decreases in the expression of GFAP by photo-activation may be due to the interaction of activated ERK and PI3K/Akt signaling with STATs and Smads signaling.

When OS3ChR2 cells were injected into mice with LPC-induced demyelination, motor function significantly recovered with injection of photo-activated OS3ChR2 cells as compared with cells without BL. In addition, photo-activated OS3ChR2 cells were not only attached to neurons but also wrapped them like myelin. These seemed that the differentiated cells helped recovery of motor function more effectively. Several studies showed activation of ERK1/2 and Akt in glial progenitor cells played important roles in the re-myelination (Gaesser and Fyffe-Maricich, 2016). As ERK1/2 and Akt signaling in OS3ChR2 cells were activated by photo-activation, re-myelination might be promoted in demyelinated mice after injection of photo-activated OS3ChR2 cells.

In conclusion, we demonstrated that signal transduction by ChR2-expressing glial progenitor cells may be controlled through alterations induced in the intracellular ion environment by photo-activation and results in oligodendrocyte differentiation from glial progenitor cells. Our results also suggest that ChR2-expressing glial progenitor cells have potential as a useful tool for therapeutic approaches to brain and spinal cord disorders associated with oligodendrocyte dysfunctions.

Acknowledgments

We thank Dr. Karl Deisseroth (Stanford University) for providing the expression vectors.

This study was supported by the Research Foundation for Opto-Science and Technology and JSPS KAKENHI Grant Number 15K18337.

The authors declare no conflict of interest.

References

Alberdi, E., Sánchez-Gómez, M.V., Matute, C., 2005. Calcium and glial cell death. Cell Calcium 38, 417–25. doi:10.1016/j.ceca.2005.06.020

Amin, A.R., Ichigotani, Y., Oo, M.L., Biswas, M.H., Yuan, H., Huang, P., Mon, N.N., Hamaguchi, M., 2003. The PLC-PKC cascade is required for IL-1β-dependent Erk and Akt activation: their role in proliferation. Int J Oncol 23, 1727–1731.

Baron, W., Metz, B., Bansal, R., Hoekstra, D., De Vries, H., 2000. PDGF and FGF-2 signaling in oligodendrocyte progenitor cells: regulation of proliferation and differentiation by multiple intracellular signaling pathways. Mol Cell Neurosci 15, 314–329.

Basso, D.M., Fisher, L.C., Anderson, A.J., Jakeman, L.B.Y.N.B., Tigue, D.M.M.C., Popovich, P.G., McTigue, D.M., Popovich, P.G., 2006. Basso Mouse Scale for locomotion detects differences in recovery after spinal cord injury in five common mouse strains. J. Neurotrauma 23, 635–659. doi:10.1089/neu.2006.23.635

Berger, T., Schnitzer, J., Orkand, P.M., Kettenmann, H., 1992. Sodium and Calcium Currents in Glial Cells of the Mouse Corpus Callosum Slice. Eur J Neurosci 4, 1271–1284.

Bernard, F., Vanhoutte, P., Bennasroune, A., Labourdette, G., Perraut, M., Aunis, D., Gaillard, S., 2006. pH is an intracellular effector controlling differentiation of oligodendrocyte precursors in culture via activation of the ERK1/2 pathway. J Neurosci Res 84, 1392–1401.

Bibollet-Bahena, O., Almazan, G., 2009. IGF-1-stimulated protein synthesis in oligodendrocyte progenitors requires PI3K/mTOR/Akt and MEK/ERK pathways. J Neurochem 109, 1440–51. doi:10.1111/j.1471-4159.2009.06071.x

Bonaguidi, M.A., McGuire, T., Hu, M., Kan, L., Samanta, J., Kessler, J.A., 2005. LIF and BMP signaling generate separate and discrete types of GFAP-expressing cells. Development 132, 5503–14.

doi:10.1242/dev.02166

Boussouf, A., Gaillard, S., 2000. Intracellular pH changes during oligodendrocyte differentiation in primary culture. J Neurosci Res 59, 731–739.

Bubner, B., Gase, K., Baldwin, I.T., 2004. Two-fold differences are the detection limit for determining transgene copy numbers in plants by real-time PCR. BMC Biotechnol 4, 14. doi:10.1186/1472-6750-4-14

Chipoy, C., Berreur, M., Couillaud, S., Pradal, G., Vallette, F., Colombeix, C., Rédini, F., Heymann, D., Blanchard, F., 2004. Downregulation of osteoblast markers and induction of the glial fibrillary acidic protein by oncostatin M in osteosarcoma cells require PKCdelta and STAT3. J Bone Min. Res 19, 1850–61. doi:10.1359/JBMR.040817

Cui, Q.L., Almazan, G., 2007. IGF-I-induced oligodendrocyte progenitor proliferation requires PI3K/Akt, MEK/ERK, and Src-like tyrosine kinases. J Neurochem 100, 1480–1493.

Dore, J.J., DeWitt, J.C., Setty, N., Donald, M.D., Joo, E., Chesarone, M.A., Birren, S.J., 2009. Multiple signaling pathways converge to regulate bone-morphogenetic-protein-dependent glial gene expression. Dev Neurosci 31, 473–86. doi:10.1159/000210187

Drouva, S. V, Faivre-Bauman, A., Loudes, C., Laplante, E., Kordon, C., 1991. Alpha 1-adrenergic receptor coupling with phospholipase-C is negatively regulated by protein kinase-C in primary cultures of hypothalamic neurons and glial cells. Endocrinology 129, 1605–13.

Figueiredo, M., Lane, S., Tang, F., Liu, B.H., Hewinson, J., Marina, N., Kasymov, V., Souslova, E.A., Chudakov, D.M., Gourine, A. V, Teschemacher, A.G., Kasparov, S., 2011. Optogenetic experimentation on astrocytes. Exp Physiol 96, 40–50. doi:10.1113/expphysiol.2010.052597

Flores, A.I., Mallon, B.S., Matsui, T., Ogawa, W., Rosenzweig, A., Okamoto, T., Macklin, W.B., 2000. Akt-mediated survival of oligodendrocytes induced by neuregulins. J Neurosci 20, 7622–30.

Frost, E.E., Zhou, Z., Krasnesky, K., Armstrong, R.C., 2009. Initiation of oligodendrocyte progenitor cell migration by a PDGF-A activated extracellular regulated kinase (ERK) signaling pathway. Neurochem Res 34, 169–81. doi:10.1007/s11064-008-9748-z

Fyffe-Maricich, S.L., Karlo, J.C., Landreth, G.E., Miller, R.H., 2011. The ERK2 mitogen-activated protein kinase regulates the timing of oligodendrocyte differentiation. J Neurosci 31, 843–850.

Gaesser, J.M., Fyffe-Maricich, S.L., 2016. Intracellular signaling pathway regulation of myelination and remyelination in the CNS. Exp Neurol 283, 501–11. doi:10.1016/j.expneurol.2016.03.008

Guardiola-Diaz, H.M., Ishii, A., Bansal, R., 2012. Erk1/2 MAPK and mTOR signaling sequentially regulates progression through distinct stages of oligodendrocyte differentiation. Glia 60, 476–86.

Hart, I.K., Richardson, W.D., Bolsover, S.R., Raff, M.C., 1989. PDGF and intracellular signaling in the timing of oligodendrocyte differentiation. J Cell Biol 109, 3411–7.

Heinrich, M., Gorath, M., Richter-Landsberg, C., 1999. Neurotrophin-3 (NT-3) modulates early differentiation of oligodendrocytes in rat brain cortical cultures. Glia 28, 244–55.

Herrera, F., Chen, Q., Schubert, D., 2010. Synergistic effect of retinoic acid and cytokines on the regulation of glial fibrillary acidic protein expression. J Biol Chem 285, 38915–22. doi:10.1074/jbc.M110.170274

Hu, X., Jin, L., Feng, L., 2004. Erk1/2 but not PI3K pathway is required for neurotrophin 3-induced oligodendrocyte differentiation of post-natal neural stem cells. J Neurochem 90, 1339–1347.

Jacinto, E., Loewith, R., Schmidt, A., Lin, S., Rüegg, M.A., Hall, A., Hall, M.N., 2004. Mammalian TOR complex 2 controls the actin cytoskeleton and is rapamycin insensitive. Nat Cell Biol 6, 1122–8. doi:10.1038/ncb1183

Le Good, J.A., Ziegler, W.H., Parekh, D.B., Alessi, D.R., Cohen, P., Parker, P.J., 1998. Protein kinase C

isotypes controlled by phosphoinositide 3-kinase through the protein kinase PDK1. Science 281, 2042–5.

McMorris, F.A., Furlanetto, R.W., Mozell, R.L., Carson, M.J., Raible, D.W., 1990. Regulation of oligodendrocyte development by insulin-like growth factors and cyclic nucleotides. Ann N Y Acad Sci 605, 101–9.

Narayanan, S.P., Flores, A.I., Wang, F., Macklin, W.B., 2009. Akt signals through the mammalian target of rapamycin pathway to regulate CNS myelination. J Neurosci 29, 6860–6870.

Nave, K.A., 2010. Myelination and support of axonal integrity by glia. Nature 468, 244–52. doi:10.1038/nature09614

Ohtani, K., Suzumura, A., Sawada, M., Marunouchi, T., Nakashima, I., Takahashi, A., 1992. Establishment of mouse oligodendrocyte/type-2 astrocyte lineage cell line by transfection with origin-defective simian virus 40 DNA. Cell Struct Funct 17, 325–333.

Ono, K., Suzuki, H., Higa, M., Tabata, K., Sawada, M., 2014. Glutamate release from astrocyte cell-line GL261 via alterations in the intracellular ion environment. J Neural Transm 121, 245–257. doi:10.1007/s00702-013-1096-8

Paez, P.M., Fulton, D., Colwell, C.S., Campagnoni, A.T., 2009. Voltage-operated Ca(2+) and Na(+) channels in the oligodendrocyte lineage. J Neurosci Res 87, 3259–66. doi:10.1002/jnr.21938

Paez, P.M., Fulton, D.J., Spreur, V., Handley, V., Campagnoni, A.T., 2010. Multiple kinase pathways regulate voltage-dependent Ca2+ influx and migration in oligodendrocyte precursor cells. J Neurosci 30, 6422–33. doi:10.1523/JNEUROSCI.5086-09.2010

Paez, P.M., Spreuer, V., Handley, V., Feng, J.M., Campagnoni, C., Campagnoni, A.T., 2007. Increased expression of golli myelin basic proteins enhances calcium influx into oligodendroglial cells. J Neurosci 27, 12690–9. doi:10.1523/JNEUROSCI.2381-07.2007

Peltier, J., O'Neill, A., Schaffer, D. V, 2007. PI3K/Akt and CREB regulate adult neural hippocampal progenitor proliferation and differentiation. Dev Neurobiol 67, 1348–61. doi:10.1002/dneu.20506

Raff, M.C., Lillien, L.E., Richardson, W.D., Burne, J.F., Noble, M.D., 1988. Platelet-derived growth factor from astrocytes drives the clock that times oligodendrocyte development in culture. Nature 333, 562–565.

Sawamura, S., Sawada, M., Ito, M., Nagatsu, T., Nagatsu, I., Suzumura, A., Shibuya, M., Sugita, K., Marunouchi, T., 1995. The bipotential glial progenitor cell line can develop into both oligodendrocytes and astrocytes in the mouse forebrain. Neurosci Lett 188, 1–4.

Schreiber, R., 2005. Ca2+ signaling, intracellular pH and cell volume in cell proliferation. J Membr Biol 205, 129–37. doi:10.1007/s00232-005-0778-z

Solà, C., Barrón, S., Tusell, J.M., Serratosa, J., 1999. The Ca2+/calmodulin signaling system in the neural response to excitability. Involvement of neuronal and glial cells. Prog Neurobiol 58, 207–32.

Sontheimer, H., 1994. Voltage-dependent ion channels in glial cells. Glia 11, 156–72. doi:10.1002/glia.440110210

Sontheimer, H., Trotter, J., Schachner, M., Kettenmann, H., 1989. Channel expression correlates with differentiation stage during the development of oligodendrocytes from their precursor cells in culture. Neuron 2, 1135–45.

Stipursky, J., Francis, D., Gomes, F.C.A., 2012. Activation of MAPK/PI3K/SMAD pathways by TGF-β(1) controls differentiation of radial glia into astrocytes in vitro. Dev Neurosci 34, 68–81. doi:10.1159/000338108

Tyler, W.A., Gangoli, N., Gokina, P., Kim, H.A., Covey, M., Levison, S.W., Wood, T.L., 2009. Activation of the mammalian target of rapamycin (mTOR) is essential for oligodendrocyte differentiation. J Neurosci 29, 6367–78. doi:10.1523/JNEUROSCI.0234-09.2009

Van't Veer, A., Du, Y., Fischer, T.Z., Boetig, D.R., Wood, M.R., Dreyfus, C.F., 2009. Brain-derived neurotrophic factor effects on oligodendrocyte progenitors of the basal forebrain are mediated through trkB and the MAP kinase pathway. J Neurosci Res 87, 69–78. doi:10.1002/jnr.21841

Zhang, F., Aravanis, A., Adamantidis, A., Lecea, L. de, Deisseroth, K., 2007. Circuit-breakers: optical technologies for probing neural signals and systems. Nat Rev Neurosci 8, 577–581. doi:10.1038/nrn2192

Zonouzi, M., Renzi, M., Farrant, M., Cull-Candy, S., 2011. Bidirectional plasticity of calcium-permeable AMPA receptors in oligodendrocyte lineage cells. Nat Neurosci 14, 1430–1438.

Figure legends

Fig. 1. OS3 cells transfected with the ChR2-EYFP gene (OS3ChR2 cells).

(A) The expression of the ChR2-EYFP fusion protein in OS3ChR2 cells was detected by FACS (A) and Western blotting (B). The filled histogram indicates EYFP fluorescence of OS3 cells and the solid line indicates fluorescence of OS3ChR2 cells.

Fig. 2. Na^+ and Ca^{2+} influx in OS3ChR2 cells by BL exposure.

Na^+ influx in OS3ChR2 cells, labeled with CoroNa Red, by BL exposure was observed using time-lapse imaging. (A) Photographs showed fluorescent images of OS3 cells and OS3ChR2 cells at 0 and 600 s with BL exposure. The scale bar indicates 50 μm. The intracellular red fluorescence of CoroNa Red was measured and the results were summarized in a graph (B). Values represent the mean ± SD. *p<0.05, **p<0.01 vs OS3 cells at the same time point. Ca^{2+} influx in OS3ChR2 cells, labeled with Rhod-3, by BL exposure was observed using time-lapse imaging. (C) Photographs showed fluorescent images of OS3 cells and OS3ChR2 cells at 0 and 600 s with BL exposure. The scale bar indicates 50 μm. The intracellular red fluorescence of Rhod-3 was measured and the results were summarized in a graph (D). Values represent the mean ± SD. *p<0.05, **p<0.01 vs OS3 cells at the same time point. (E) The intracellular red fluorescence of CoroNa red was measured in sodium ion-free buffer (Na^+ free) or in RB in the presence or absence of EGTA (100 μM) at 0-600 s with BL and alterations in fluorescence during 10 min were summarized in a graph. (F) The intracellular red fluorescence of Rhod-3 was measured in sodium ion-free buffer (Na^+ free) or in RB in the presence or absence of EGTA (100 μM), BAPTA-AM (10 μM) and Ionomycin (1 μM) at 0-600 s with BL and alterations in fluorescence during 10 min were summarized in a graph. Values represent the mean ± SD. **p<0.01, ***p<0.001 vs OS3 cells with BL. ##p<0.01, ###p<0.001 vs OS3ChR2 cells with BL. (G) The intracellular red fluorescence of CoroNa Red and Rhod-3 was measured at 0 and 72 h with

BL and alterations in fluorescence during 72 h were summarized in a graph. Values represent the mean ± SD. ***p<0.001 vs OS3ChR2 cells without BL (N).

Fig. 3. Differentiation of OS3ChR2 cells into oligodendrocytes by photo-activation.

The mRNA expression of differentiation markers such as PLP, Olig2, GFAP, Cx43, and GLAST was examined in OS3 and OS3ChR2 cells with BL or without BL exposure (N) (A). Values represent the mean ± SD. **p<0.01, ***p<0.001 vs OS3ChR2 N. The protein expression of GalC and GFAP was detected in OS3ChR2 cells at 0, 1 and 3 days with BL exposure by FACS analysis (B). In addition, the protein expression of GalC and GFAP was also detected in OS3 and OS3ChR2 N or BL by Western blotting (C). Each expression was summarized in graphs. Values represent the mean ± SD. **p<0.01, ***p<0.001 vs OS3ChR2 N. The protein expression of GalC and GFAP was also detected in OS3ChR2 cells in the presence or absence of EGTA (100 μM) (D) or BAPTA-AM (10 μM) (E) with BL or N by Western blotting. Each expression was summarized in graphs. Values represent the mean ± SD. *p<0.05, **p<0.01, ***p<0.001 vs OS3ChR2 N. $^{###}$p<0.001 vs OS3ChR2 BL.

Fig. 4. GalC expression in OS3ChR2 cells by photo-activation was not involved in the phosphorylation of ERK1/2.

The phosphorylation of MAPKs such as ERK1/2, p38 MAPK, and JNK was detected in OS3ChR2 cells at 0-24 h with BL exposure by Western blotting (A). The ratio of phosphorylated ERK1 and 2 was summarized in a graph. Values represent the mean ± SD. **p<0.01, ***p<0.001 vs OS3ChR2 cells at 0 h with BL. The phosphorylation of ERK1/2 was also detected in OS3ChR2 cells at 6 h in the presence or absence of U0126 (1 μM) with or without BL (B). The ratio of phosphorylated ERK1 and 2 was summarized in a graph. Values represent the mean ± SD. **p<0.01, ***p<0.001 vs OS3ChR2 N. $^{###}$p<0.001 vs OS3ChR2 BL. The protein expression of GalC and GFAP was examined

in OS3ChR2 cells at 72 h in the presence or absence of U0126 (1 μM) with or without BL, respectively (C). Values represent the mean ± SD. **p<0.01, ***p<0.001 vs OS3ChR2 N. ###p<0.001 vs OS3ChR2 BL.

Fig. 5. The phosphorylation of ERK1/2 in OS3ChR2 cells by photo-activation was required for cell growth and survival.

The phosphorylation of ERK1/2 was examined in OS3ChR2 cells at 6 h in the presence of EGTA (100 μM) (A) or BAPTA-AM (10 μM) (B) with or without BL. Values represent the mean ± SD. ***p<0.001 vs OS3ChR2 N, ###p<0.001 vs OS3ChR2 BL. The proliferation of OS3ChR2 cells was investigated on Days 1 and 3 in the presence of U0126 (0-10 μM) with or without BL exposure by the WST assay (C). Values represent the mean ± SD. *p<0.05, **p<0.01, ***p<0.001 vs OS3ChR2 cells in the absence of U0126 without BL. ###p<0.001 vs OS3ChR2 cells in the absence of U0126 with BL. The viability of OS3ChR2 cells on Day 3 in the presence of U0126 (0-10 μM) with or without BL exposure was summarized in a graph (D). Values represent the mean ± SD. ***p<0.001 vs OS3ChR2 cells in the absence of U0126 without BL. ###p<0.001 vs OS3ChR2 cells in the absence of U0126 with BL.

Fig. 6. Phosphorylation of Akt in OS3ChR2 cells by photo-activation.

The phosphorylation of Akt and PDK1 was detected in OS3ChR2 cells at 0-24 h with BL exposure (A). The ratio of phosphorylated Akt or PDK1 was summarized in a graph. Values represent the mean ± SD. *p<0.05, **p<0.01, ***p<0.001 vs OS3ChR2 cells at 0 h with BL. The phosphorylation of Akt and PDK1 was examined in OS3ChR2 cells at 6 h in the presence or absence of EGTA (100 μM) (B) or BAPTA-AM (10 μM) (C) with or without BL. The ratio of phosphorylated Akt or PDK1 was summarized in a graph. Values represent the mean ± SD. *p<0.05, **p<0.01, ***p<0.001 vs

OS3ChR2 N. ###p<0.001 vs OS3ChR2 BL.

Fig. 7. GalC expression in OS3ChR2 cells by photo-activation was involved in the phosphorylation of Akt and PDK1.

The phosphorylation of Akt was detected in OS3ChR2 cells at 6 h in the presence or absence of LY294002 (10 μM), Triciribine (1 μM), and BX-517 (1 μM) with or without BL (A). The ratio of phosphorylated Akt was summarized in a graph. Values represent the mean ± SD. The protein expression of GalC and GFAP was analyzed in OS3ChR2 cells at 72 h in the presence or absence of LY294002 (10 μM), Triciribine (1 μM), and BX-517 (1 μM) with or without BL, respectively (B). Values represent the mean ± SD. *p<0.05, **p<0.01, ***p<0.001 vs OS3ChR2 cells in the absence of LY294002, Triciribine, and BX-517 without BL. ##p<0.01, ###p<0.001 vs OS3ChR2 cells in the absence of LY294002, Triciribine, and BX-517 with BL.

Fig. 8. GalC expression in OS3ChR2 cells by photo-activation was involved in the phosphorylation of mTOR and p70 S6K.

The phosphorylation of mTOR on Ser2448 (A) and p70S6K on Thr389 and Ser371 (C) in OS3ChR2 cells in the presence or absence of rapamycin (50 nM) for 6 h with or without BL was detected by Western blotting. The expression of GalC and GFAP in OS3ChR2 cells in the presence or absence of rapamycin (50 nM) for 72 h with or without BL was also detected by Western blotting (B). Phosphorylation and expression were summarized in graphs. Values represent the mean ± SD. *p<0.05, **p<0.01, ***p<0.001 vs OS3ChR2 cells N. ###p<0.001 vs OS3ChR2 BL.

Fig. 9. Photo-activated OS3ChR2 cells recovered motor function in demyelinated mice.

Motor function recovery was evaluated with BMS score (A) and rota-rod test (B) at 0-2 weeks after

cell injection. Values represent the mean ± SD. **p<0.01, ***p<0.001 vs LPC_No cells. $^{\#}$p<0.05, $^{\#\#}$p<0.01, $^{\#\#\#}$p<0.001 vs LPC_OS3ChR2N. (C) Thoracic spinal cord sections with LFB staining at 2 weeks after cell injection. (D) Representative results of immunohistochemical assay for MAP-2 (red) and ChR2 (green). Scale bar indicates 50 μm. Right panel shows a high-power field confocal image of a region in left panel. (E) Percentage of GalC-expressing cells in OS3ChR2 cells in the spinal cord was measured $^{\#\#\#}$p<0.001 vs OS3ChR2N. Vehicle; PBS treatment, LPC_No cells; LPC treatment and injection of no cells, LPC_OS3ChR2N; LPC treatment and injection of OS3ChR2 cells without BL exposure, LPC_OS3ChR2BL; LPC treatment and injection of OS3ChR2 cells with BL exposure.

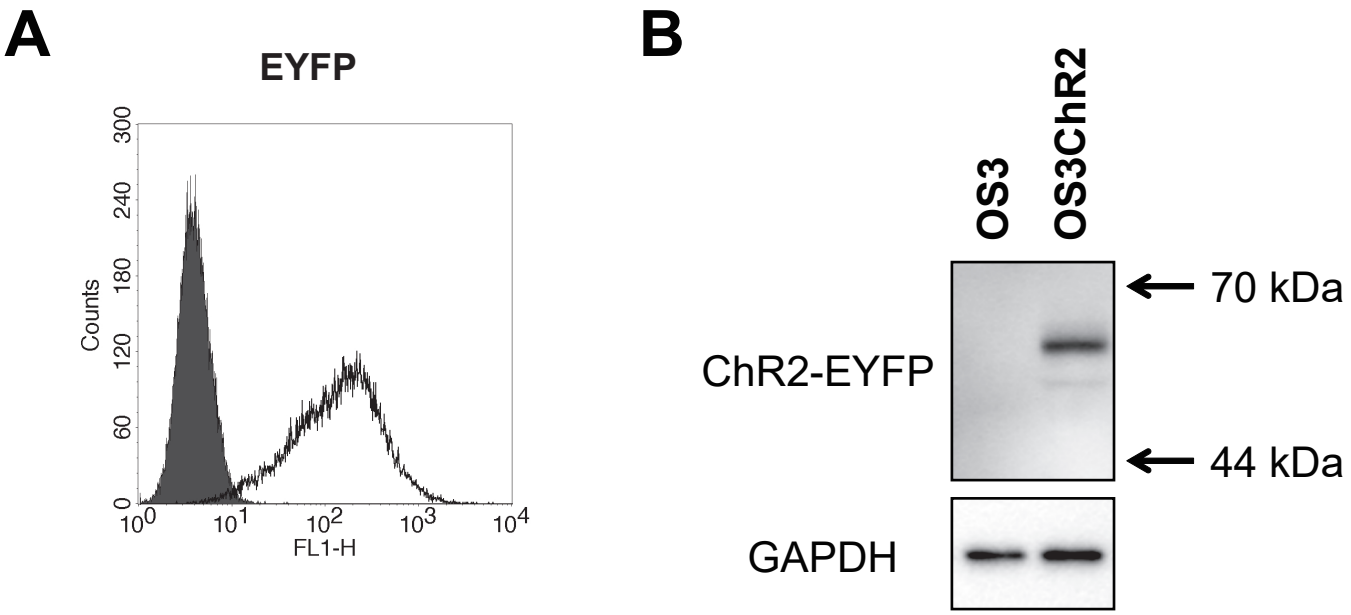
A
EYFP
Counts
0
60
120
180
240
300
10^0
10^1
10^2
10^3
10^4
FL1-H
B
OS3
OS3ChR2
70 kDa
ChR2-EYFP
44 kDa
GAPDH

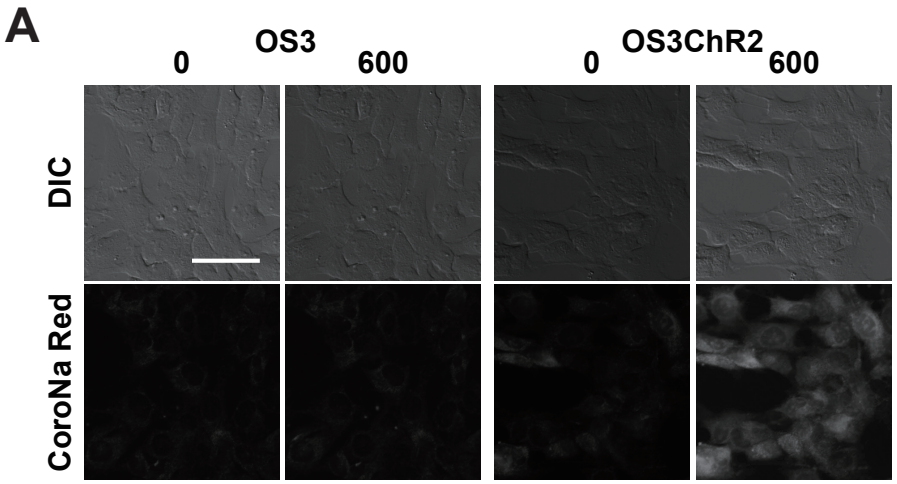
A
OS3
0
600
OS3ChR2
0
600
DIC
CoroNa Red

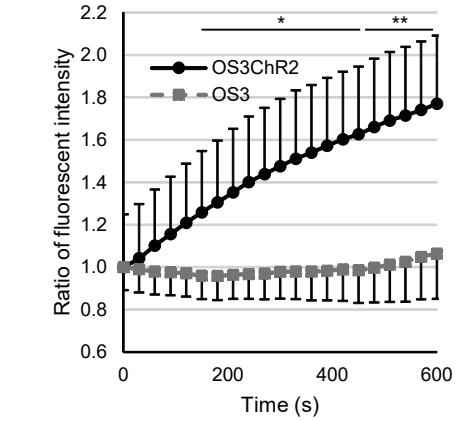
B
Ratio of fluorescent intensity
OS3ChR2
OS3
Time (s)

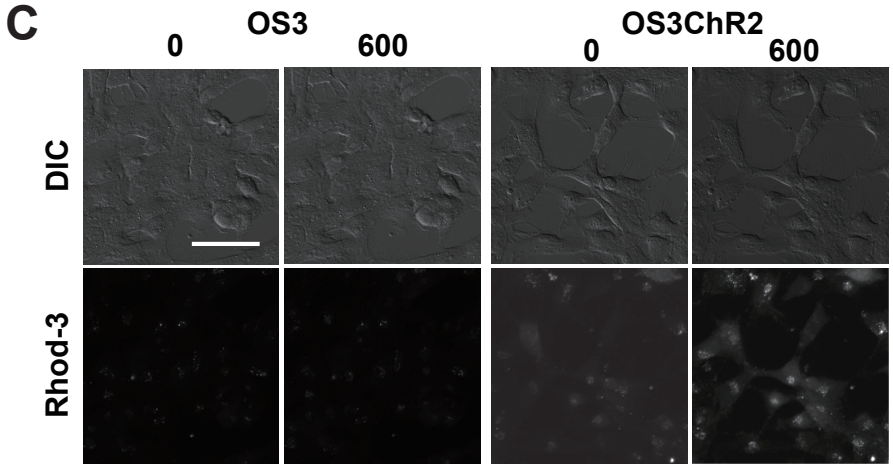
C
OS3
0
600
OS3ChR2
0
600
DIC
Rhod-3

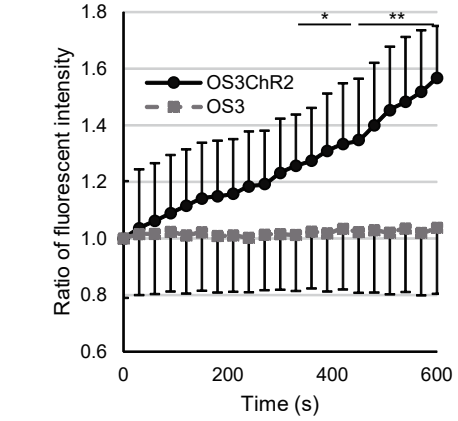
D
Ratio of fluorescent intensity
OS3ChR2
OS3
Time (s)

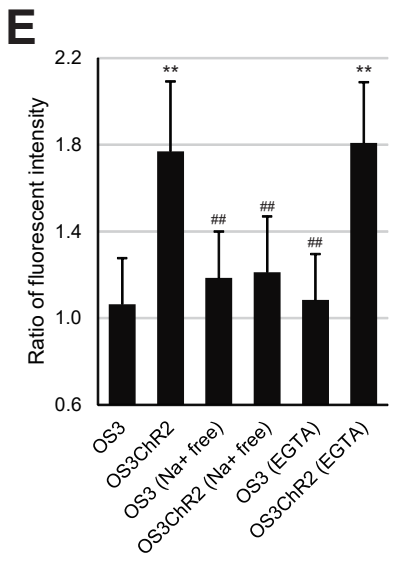
E
Ratio of fluorescent intensity
OS3
OS3ChR2
OS3 (Na+ free)
OS3ChR2 (Na+ free)
OS3 (EGTA)
OS3ChR2 (EGTA)

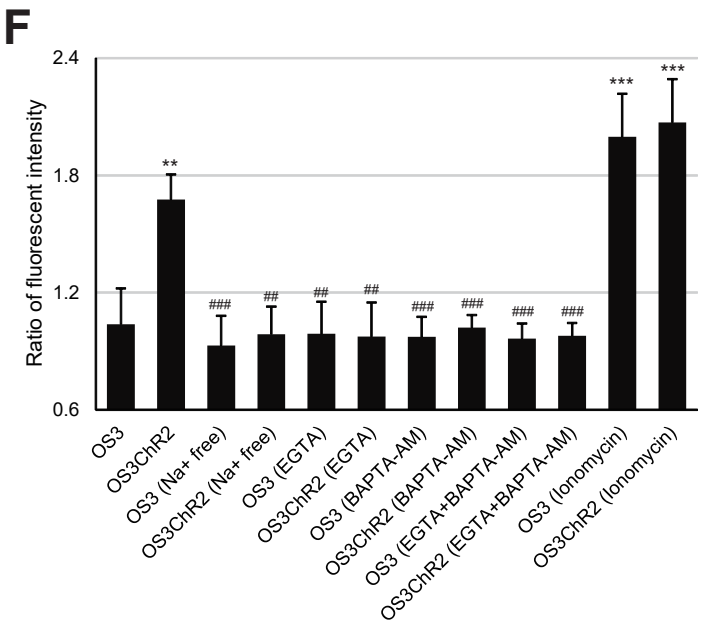
F
Ratio of fluorescent intensity
OS3
OS3ChR2
OS3 (Na+ free)
OS3ChR2 (Na+ free)
OS3 (EGTA)
OS3ChR2 (EGTA)
OS3 (BAPTA-AM)
OS3ChR2 (BAPTA-AM)
OS3 (EGTA+BAPTA-AM)
OS3ChR2 (EGTA+BAPTA-AM)
OS3 (Ionomycin)
OS3ChR2 (Ionomycin)

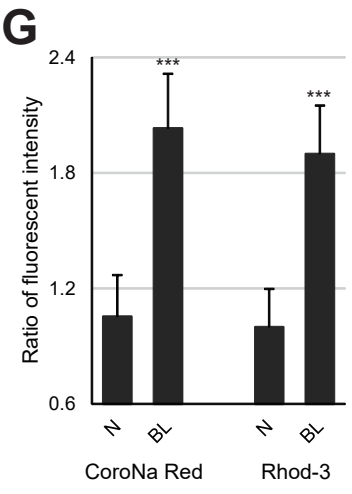
G
Ratio of fluorescent intensity
N
BL
N
BL
CoroNa Red
Rhod-3

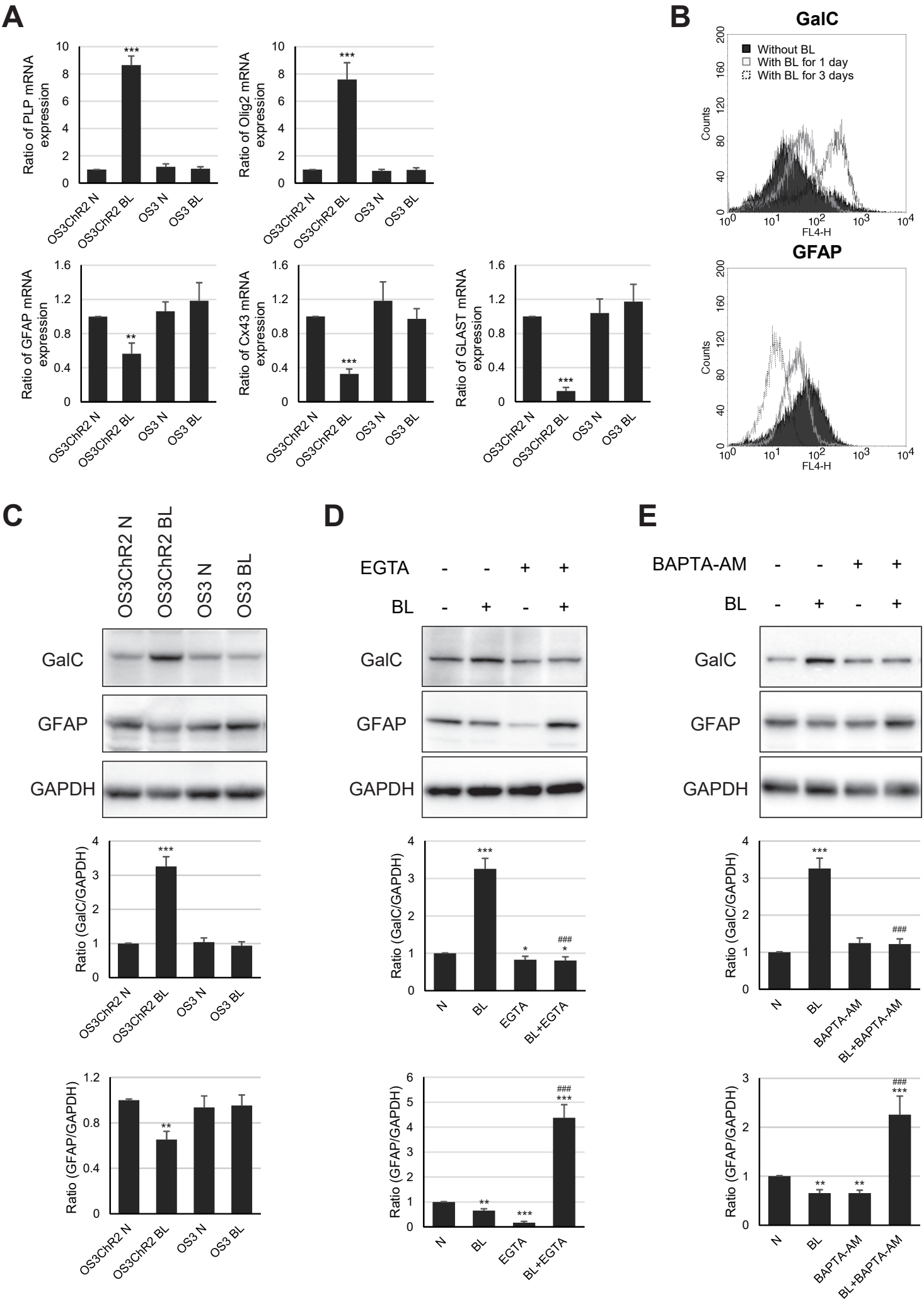
A
Ratio of PLP mRNA expression
Ratio of Olig2 mRNA expression
Ratio of GFAP mRNA expression
Ratio of Cx43 mRNA expression
Ratio of GLAST mRNA expression
OS3ChR2 N
OS3ChR2 BL
OS3 N
OS3 BL
B
GalC
Without BL
With BL for 1 day
With BL for 3 days
Counts
FL4-H
GFAP
C
GalC
GFAP
GAPDH
Ratio (GalC/GAPDH)
Ratio (GFAP/GAPDH)
D
EGTA
BL
N
BL
EGTA
BL+EGTA
E
BAPTA-AM
BL
N
BL
BAPTA-AM
BL+BAPTA-AM

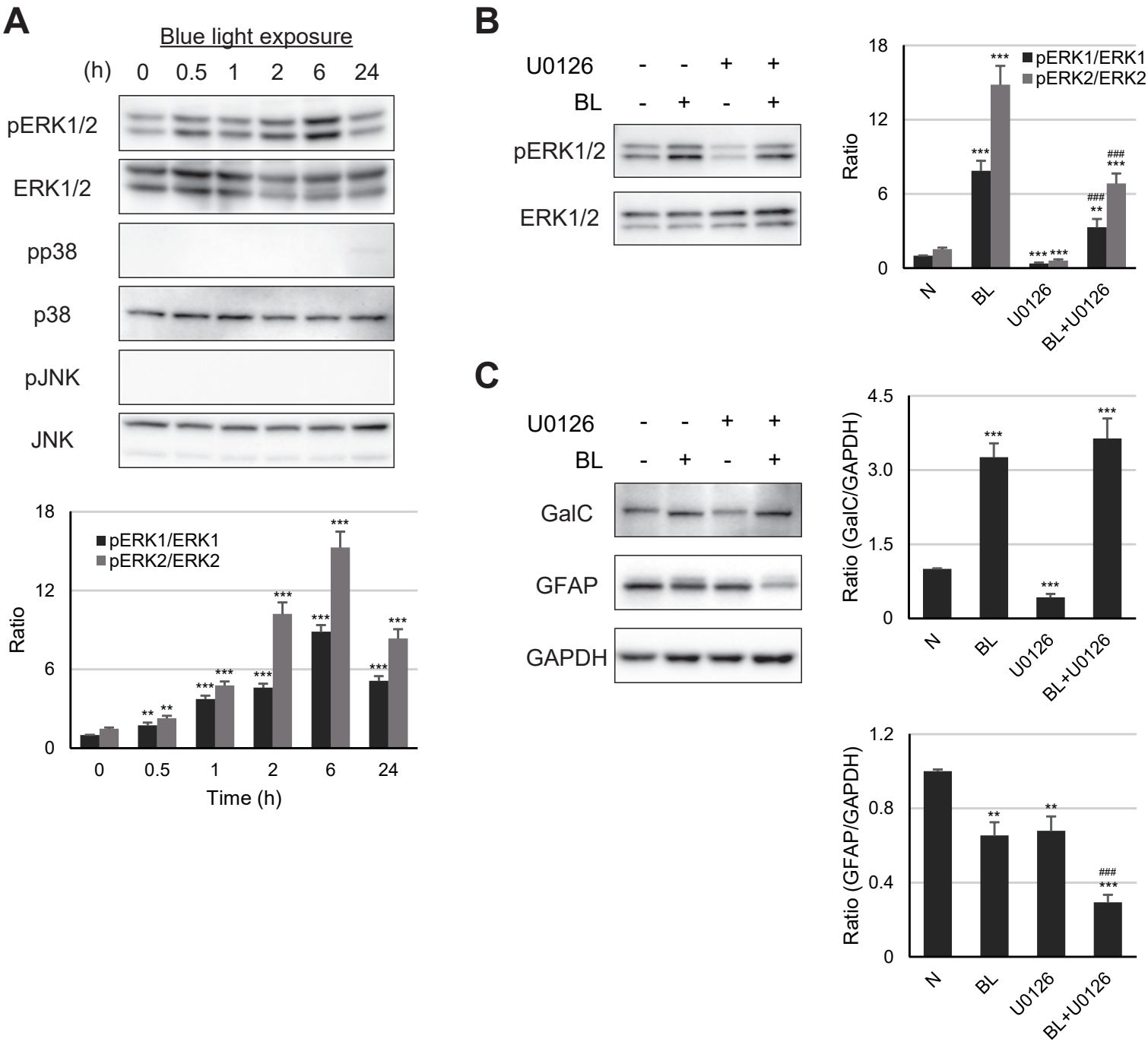
A
Blue light exposure
(h) 0 0.5 1 2 6 24
pERK1/2
ERK1/2
pp38
p38
pJNK
JNK
pERK1/ERK1
pERK2/ERK2
Ratio
Time (h)
B
U0126 - - + +
BL - + - +
pERK1/2
ERK1/2
pERK1/ERK1
pERK2/ERK2
Ratio
N
BL
U0126
BL+U0126
C
U0126 - - + +
BL - + - +
GalC
GFAP
GAPDH
Ratio (GalC/GAPDH)
Ratio (GFAP/GAPDH)

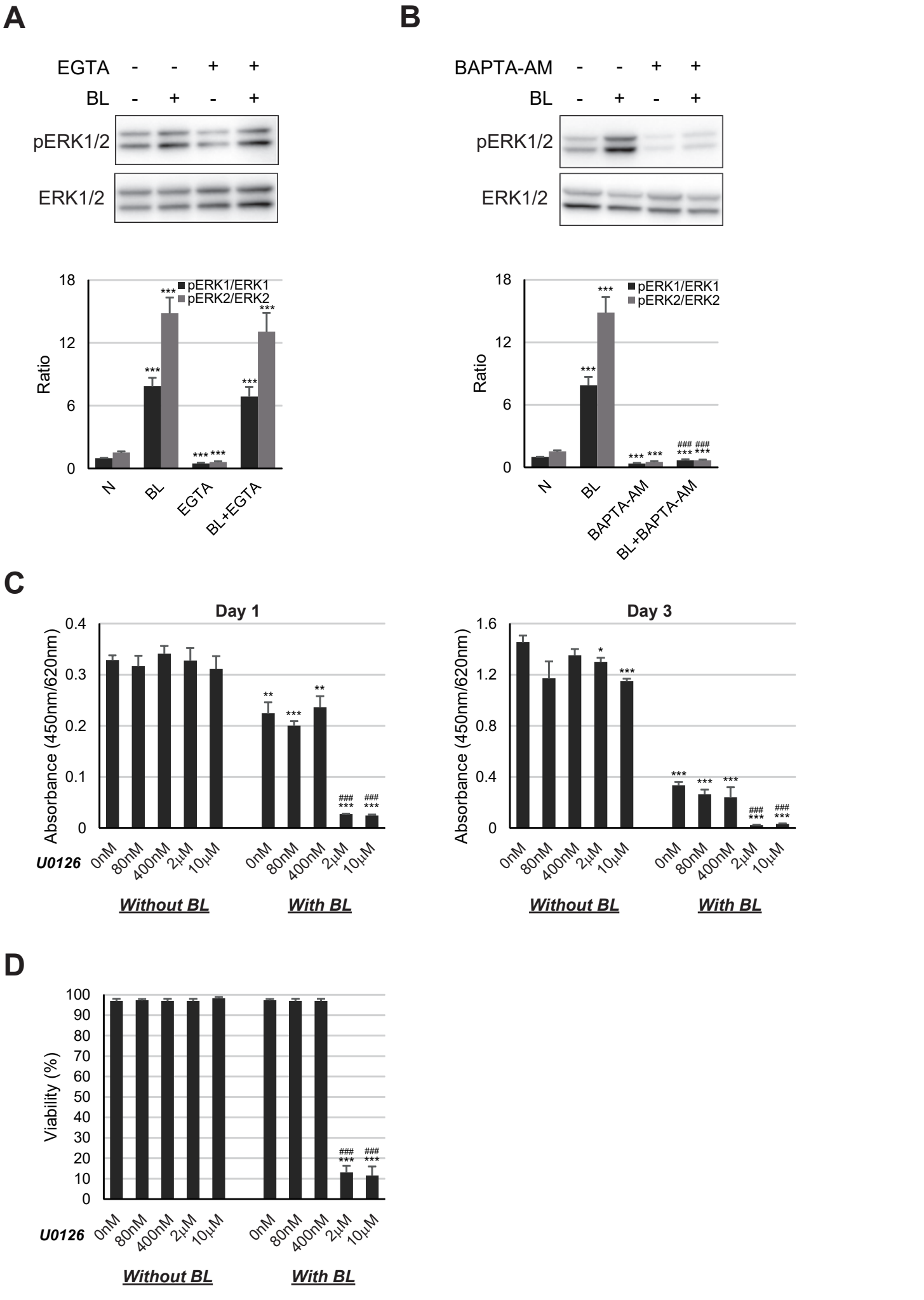
A
EGTA - - + +
BL - + - +
pERK1/2
ERK1/2
Ratio
pERK1/ERK1
pERK2/ERK2
N
BL
EGTA
BL+EGTA
B
BAPTA-AM - - + +
BL - + - +
pERK1/2
ERK1/2
Ratio
pERK1/ERK1
pERK2/ERK2
N
BL
BAPTA-AM
BL+BAPTA-AM
C
Day 1
Absorbance (450nm/620nm)
U0126 0nM 80nM 400nM 2μM 10μM 0nM 80nM 400nM 2μM 10μM
Without BL
With BL
Day 3
Absorbance (450nm/620nm)
U0126 0nM 80nM 400nM 2μM 10μM 0nM 80nM 400nM 2μM 10μM
Without BL
With BL
D
Viability (%)
U0126 0nM 80nM 400nM 2μM 10μM 0nM 80nM 400nM 2μM 10μM
Without BL
With BL

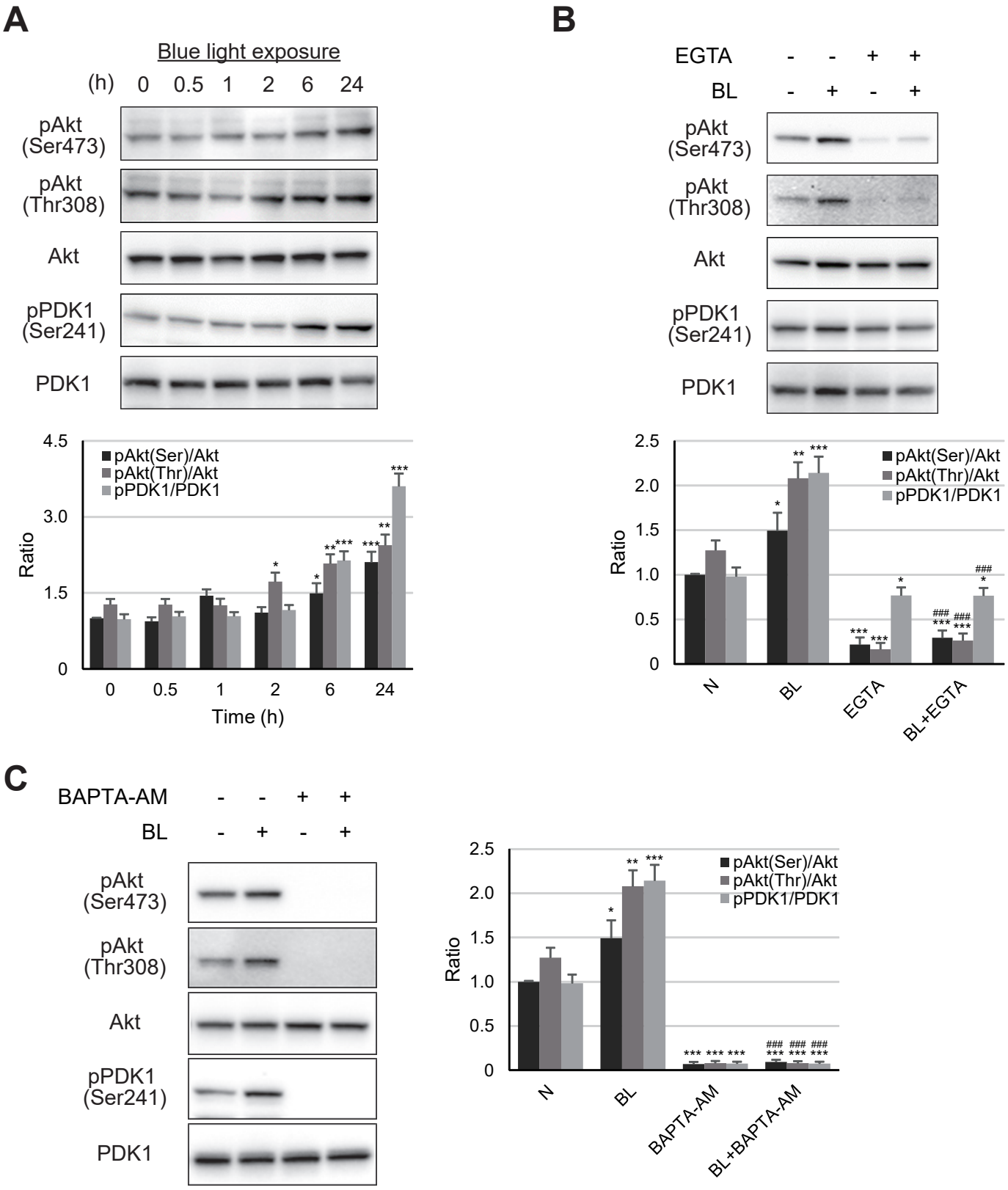
A
Blue light exposure
(h) 0 0.5 1 2 6 24
pAkt (Ser473)
pAkt (Thr308)
Akt
pPDK1 (Ser241)
PDK1
Ratio
pAkt(Ser)/Akt
pAkt(Thr)/Akt
pPDK1/PDK1
Time (h)
B
EGTA - - + +
BL - + - +
N
BL
EGTA
BL+EGTA
C
BAPTA-AM - - + +
BL - + - +
BAPTA-AM
BL+BAPTA-AM

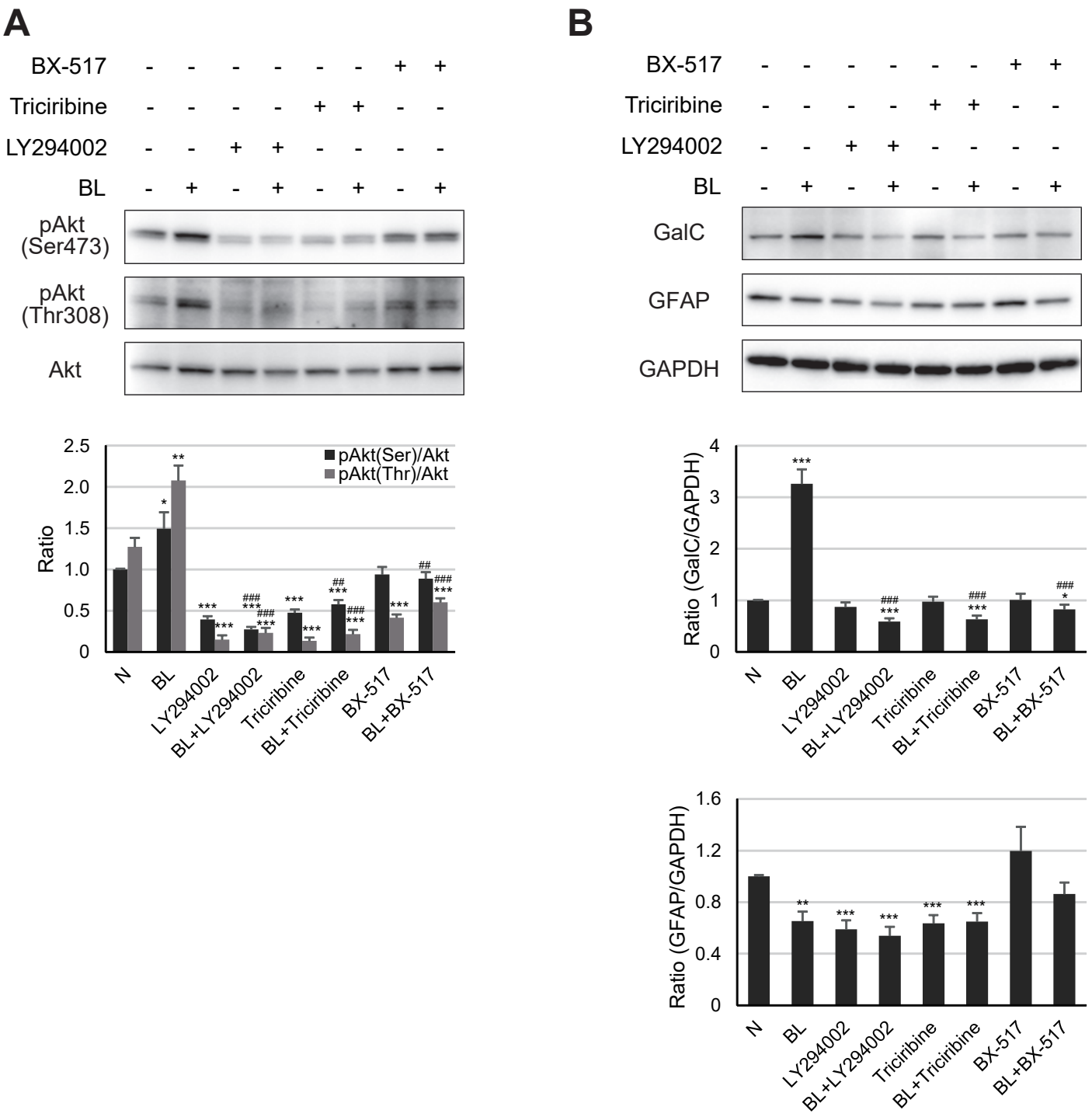
A
BX-517 - - - - - - + +
Triciribine - - - - + + - -
LY294002 - - + + - - - -
BL - + - + - + - +
pAkt (Ser473)
pAkt (Thr308)
Akt
pAkt(Ser)/Akt
pAkt(Thr)/Akt
Ratio
N
BL
LY294002
BL+LY294002
Triciribine
BL+Triciribine
BX-517
BL+BX-517
B
BX-517 - - - - - - + +
Triciribine - - - - + + - -
LY294002 - - + + - - - -
BL - + - + - + - +
GalC
GFAP
GAPDH
Ratio (GalC/GAPDH)
Ratio (GFAP/GAPDH)
N
BL
LY294002
BL+LY294002
Triciribine
BL+Triciribine
BX-517
BL+BX-517

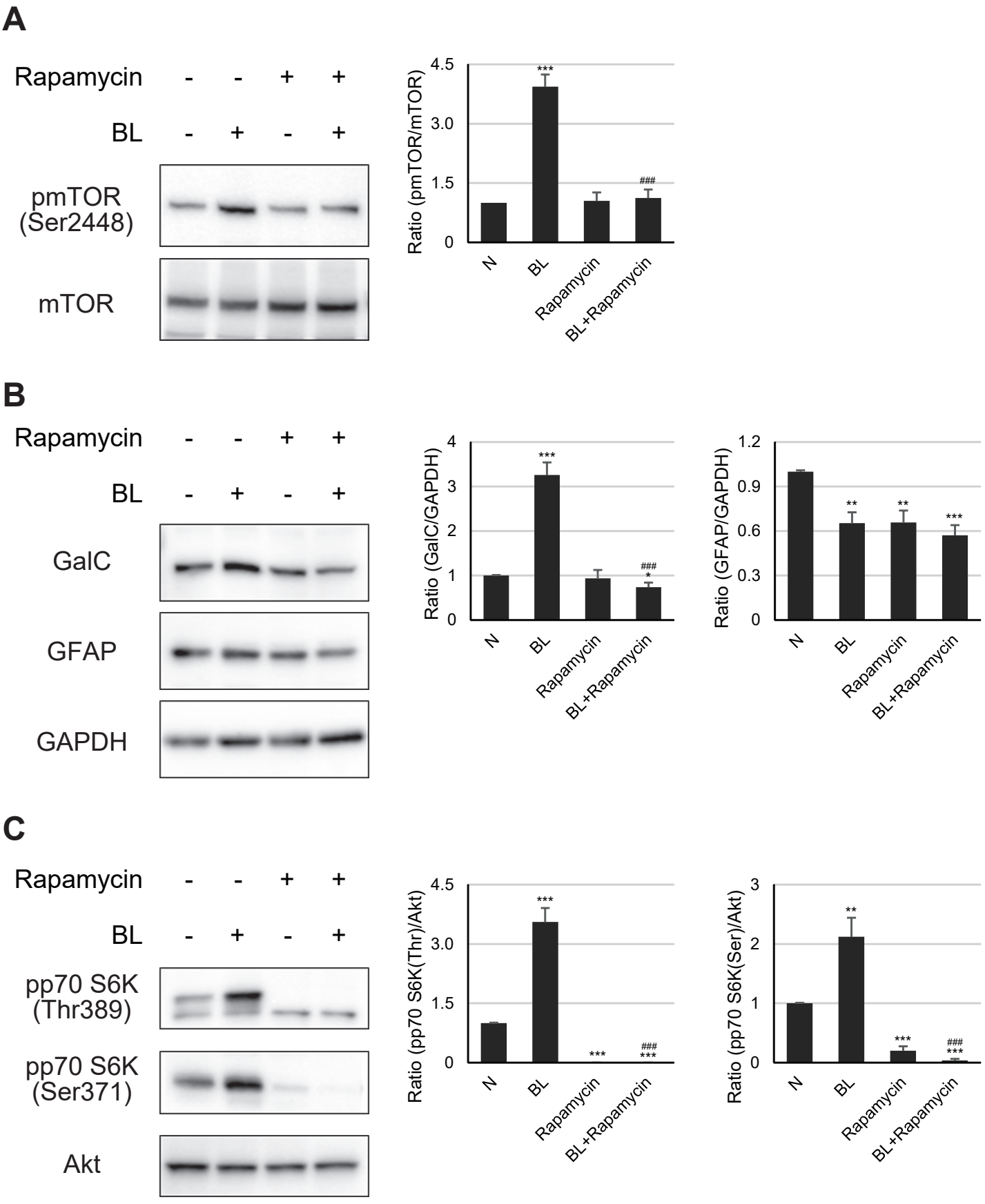
A
Rapamycin - - + +
BL - + - +
pmTOR (Ser2448)
mTOR
Ratio (pmTOR/mTOR)
4.5
3.0
1.5
0
***
###
N
BL
Rapamycin
BL+Rapamycin
B
Rapamycin - - + +
BL - + - +
GalC
GFAP
GAPDH
Ratio (GalC/GAPDH)
4
3
2
1
0
***
###
*
Ratio (GFAP/GAPDH)
1.2
0.9
0.6
0.3
0
**
**
***
C
Rapamycin - - + +
BL - + - +
pp70 S6K (Thr389)
pp70 S6K (Ser371)
Akt
Ratio (pp70 S6K(Thr)/Akt)
4.5
3.0
1.5
0
***
***
###
Ratio (pp70 S6K(Ser)/Akt)
3
2
1
0
**
***
###
***

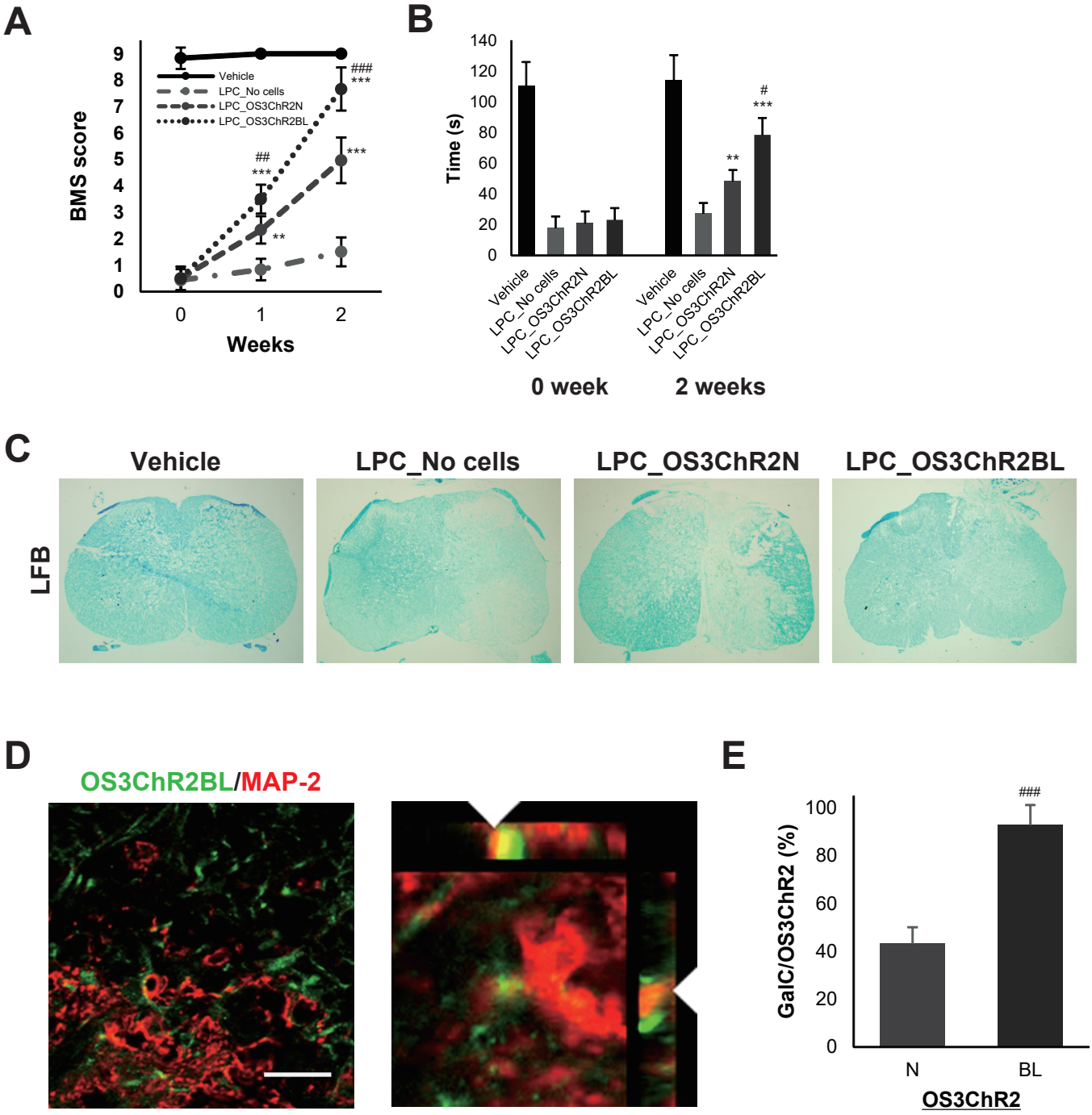
A
BMS score
Weeks
Vehicle
LPC_No cells
LPC_OS3ChR2N
LPC_OS3ChR2BL
B
Time (s)
0 week
2 weeks
C
Vehicle
LPC_No cells
LPC_OS3ChR2N
LPC_OS3ChR2BL
LFB
D
OS3ChR2BL/MAP-2
E
GalC/OS3ChR2 (%)
N
BL
OS3ChR2